Coordination Chemistry Reviews, 91 (1988) 35–88
Elsevier Science Publishers B.V., Amsterdam – Printed in The Netherlands

THE MOLECULAR GEOMETRY OF GAS-PHASE METAL HALIDES

MAGDOLNA HARGITTAI

Structural Chemistry Research Group of the Hungarian Academy of Sciences, Eötvös University, Budapest, VIII, Puskin utca 11–13, P.O. Box 117, H-1431 (Hungary)

(Received 21 December 1987)

CONTENTS

0010-8545/88/$18.90

A. INTRODUCTION

The geometry of a molecule can be characterized on two levels. The first, a more qualitative level, is simply the shape and symmetry of the molecule. Although this may seem to be trivial, it will be shown throughout this paper that even for the simplest metal halide molecules it is not actually so. This is intriguing indeed in an age when the structures of extremely complicated macromolecules are known often with great accuracy.

"The question as to whether a given triatomic molecule is linear or bent is certainly among the simplest problems in polyatomic geometry." This statement is cited from a paper on the geometry of high temperature molecular species published more than two decades ago [1]. Ensuing progress since has proved this question to be not so simple after all. Each of the available techniques has its difficulties in this respect, and will be mentioned briefly later in this review.

The second, more thorough level of molecular geometry, refers to its metrical aspects, i.e. its bond lengths, bond angles and torsional angles. Different experimental techniques provide different information about molecular geometry; they will be mentioned briefly.

There are several features that make the study of metal halides rather difficult and therefore a challenge to the structural chemist.

Most metal halides have low volatility and their gas phase investigation requires high temperature experimental conditions [2,3].

The complicated vapor composition is another experimental difficulty. It has been shown by different methods [4–7], and in particular by mass spectrometry [7] that the vapors of metal halides are often rich in a variety of different molecular species, and their composition is sensitive to temperature [8].

The highly corrosive nature of metal halides adds to the experimental difficulties. The sample may react with the container, producing further vapor phase halides. An example is quoted from ref. 9 where it is suggested that the ν_3 frequency assigned earlier to $CrCl_2$ [10] may be due to $FeCl_2$ originating from the container material. The good complexing ability of many metal chlorides is a disadvantage in this respect. Aluminum trichloride and iron trichloride are good complexing agents with most other metal halides and thus enhance the volatility of those halides by many orders of

magnitude. For this reason stainless steel, otherwise a common and accessible nozzle material for electron diffraction, is often inadequate for high temperature experiments.

Small traces of other halides in a given sample may also evaporate either by themselves or in the form of mixed complex halides, and may be present in higher concentration in the vapor than in the original solid sample. In this way they may falsify the experimental results, if they remain undetected.

(i) Experimental techniques

(a) Spectroscopic methods

As far as the structural information of molecules is concerned, vibrational and rotational spectroscopy are of special interest.

Vibrational spectroscopy is, in principle, an ideal method for obtaining information on molecular symmetry since the selection rules will often be different for different possible molecular configurations. As an example, let us consider MX_2 and MX_3 metal halides, for which the selection rules are different for linear vs. bent and planar vs. pyramidal configurations, both in IR and Raman spectroscopy. Nevertheless, several problems may make the determination of the symmetry of such molecules ambiguous. Absorptions other than fundamental transitions alone occur in the high temperature gas-phase spectra, and the relatively broad bands make assignment of these spectra difficult and less reliable.

Such problems do not arise in matrix isolation spectra where absorption bands are narrow and sharp. There are other problems though. First, the absorption frequencies are usually shifted compared with the gas phase values. For higher frequencies this is not so crucial, whereas for very low frequencies, which are often characteristic of small metal halide molecules, the relative magnitude of these shifts may be considerable. The bending frequency of a first-row transition metal dichloride, for example, falls into the region of about 50–100 cm^{-1} and the magnitude of the matrix shift may easily amount to 10–20 cm^{-1}.

Thermodynamic calculations, among others, are sensitive to the value of the ν_2 bending frequency. Moreover, these bending frequencies are often unavailable since they fall into the far-IR region. The possibility of matrix site effects should also be kept in mind. Perturbations by the matrix environment may cause a linear molecule to bend as discussed in ref. 11. Similarly, an otherwise planar molecule may appear pyramidal in certain matrices. Thus $CrCl_3$, for example, was found to be planar in an argon matrix while it was interpreted to be pyramidal in N_2 [9].

Chemical reactions may occur during deposition, producing new molecules and causing new lines to appear in the spectra. A matrix isolation IR

spectroscopic investigation of $AlCl_3$ originally reported a pyramidal geometry based on the observation of the ν_1 symmetric stretching frequency [12]. Eventually, however, the formation of an addition compound, $AlCl_3 \cdot N_2$, was supposed to cause this frequency as nitrogen was the carrier gas in the purification of the sample [13]. Thus, this complex may have given rise to a spectrum line which was interpreted as the ν_1 stretching frequency of $AlCl_3$.

The presence of different molecular species in the vapor may also hinder the interpretation of the spectra. The bands of monomers and dimers often overlap. The appearance of a dimer band in the ν_1 symmetric stretching frequency region in the IR spectrum of a linear dihalide molecule, may, for example, be incorrectly interpreted as a sign of bent geometry. Bearing in mind the possibility of complex vapor composition and taking spectra at different temperatures, and examining the changes in intensities, may facilitate their assignment. The combination of different methods, such as mass spectrometry and IR spectroscopy for the determination of vapor composition and molecular symmetry is especially advantageous.

The bond angle of a bent molecule can be determined by isotopic substitution from isotopic shifts of the asymmetric stretching frequency ν_3 in the IR spectrum [14]. This method has been shown, however, not to be sensitive enough for nearly linear configurations (cf. for example refs. 2 (a) and 14). Also, the absence of the ν_1 symmetric stretching frequency in the IR spectrum does not necessarily mean that the molecule is linear; sometimes the respective band is simply too weak to be identified.

The study of the rotational spectra of molecules is one of the best ways to obtain information about the geometrical parameters of a molecule. Microwave spectroscopy is the most important technique in this respect. Unfortunately, only molecules with a permanent electric dipole can be studied by this technique. Thus most of the simple metal halides, with their high symmetry (linear, $D_{\infty h}$, planar, D_{3h}, tetrahedral, T_d, dimers with D_{2h} and trimers with D_{3h} symmetry) are not suitable objects. A major difficulty with microwave spectroscopy at high temperatures is the population of many rotational and vibrational levels leading to a forest of lines incapable of analysis. The alkali metal halides and other monohalides are practically the only metal halides that have been studied by this technique.

(b) Electron diffraction

This is an excellent technique for determining the geometrical parameters of a molecule. Higher symmetry makes the determination of the geometrical parameters easier with this technique in contrast with microwave spectroscopy. However, the determination of molecular symmetry is sometimes difficult or ambiguous employing electron diffraction alone. Many of the early electron diffraction studies on metal halides determined molecular

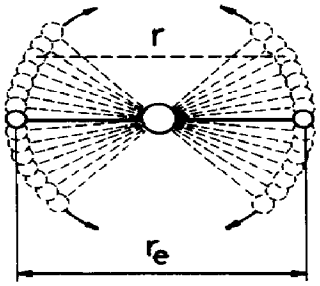

Fig. 1. Illustration of the origin of the shrinkage effect in a linear triatomic molecule.

symmetry erroneously owing to inadequacies of the early technique. The alkaline earth dihalides are examples, whose geometry was reported to be linear in early studies (for references see ref. 15). Since then it has become clear that not all of these dihalides are linear (see later in this review). Some X · · · X contributions could not be measured because of the large difference in the atomic numbers of the metal and the halogen. The determination of the symmetry for such molecules as MX_2 or MX_3, however, presents a challenge even to modern electron diffraction.

This technique determines the atom–atom contributions to electron scattering and these contributions are thermal averages. The metal halide molecules generally have very low bending or puckering mode frequencies and undergo large-amplitude motion. They are often referred to as "floppy" molecules. Electron diffraction provides an average picture of the molecules being distributed on the bending and puckering potential surfaces; thus even a linear or a planar molecule will appear to be bent or pyramidal. Beattie and Greenhalgh [2(b)] pointed out that this is also a philosophical question. Chemists wish to categorize these molecules conveniently as linear or planar, whereas they actually spend most of their time in a bent or pyramidal configuration. Figure 1 illustrates this for a linear molecule.

As a consequence of bending vibrations, the average X · · · X distance of a linear MX_2 molecule appears to be shorter than twice the M–X bond length. This is called the shrinkage effect (see for example ref. 16), and it makes the apparent bond angle of a linear MX_2 molecule smaller than 180°. Similarly, the puckering vibrations make the apparent bond angle of a planar MX_3 molecule smaller than 120°. In such cases it is impossible to distinguish between truly linear and planar molecules on the one hand and bent and pyramidal molecules on the other by electron diffraction alone.

This disadvantage may be turned into an advantage if at least some limited amount of additional data are available. Information on bending and puckering frequencies can facilitate an unambiguous choice between linear and bent as well as between planar and pyramidal geometries.

Conversely, unambiguous knowledge of a linear equilibrium configuration may lead to the estimation of vibrational quantities from the electron diffraction data.

(c) Electric deflection of molecular beam

Another qualitative method for the investigation of the symmetry of simple high temperature molecules is the molecular beam electric deflection experiment [1]. The possible origin of a dipole moment appearing for a highly symmetric molecule, however, has also been discussed [17].

(d) Quantum chemical calculations

This method is rapidly gaining recognition for the determination of molecular structure. Unfortunately, the size of the atoms often poses a problem in the study of metal halides. The larger the size and number of the atoms in a molecule, the more complicated and time consuming the calculation of molecular energy and geometry will be. The problem of electron correlation also becomes increasingly important. There are many ways to construct basis function sets for these molecules, and the results may strongly depend on them [18]. Systematic studies have already been carried out for lighter atoms, and a number of generally applicable methods and basis sets have been developed. Another difficulty arises for transition metal compounds owing to the open-shell electronic structure of the metal atom. No systematic investigation has been carried out yet on these systems, and generally acceptable calculation procedures and optimal basis sets have not yet been developed. New development is anticipated in the near future in this area.

Of course, the physical meaning of the geometrical parameters determined by calculation is different from the electron diffraction geometry. Quantum chemical calculations yield the symmetry and geometry of the hypothetical, motionless molecule, corresponding to the minimum position of the potential energy function. This is called the equilibrium geometry.

The electron diffraction geometry is a thermal average, effective structure. The symmetry of high temperature molecules often appears to be lower from electron diffraction than the equilibrium symmetry due to shrinkage effects. In addition to previous examples, the consequences of puckering in different planar halogen-bridged ring structures are mentioned here for Al_2Cl_6, Fe_2Cl_4 and Cu_3Cl_3. Figure 2 illustrates the possible lowering of symmetry as it appears in electron diffraction determinations of various molecule types.

(e) Combination of techniques

Concerted use of various techniques seems to be the most promising

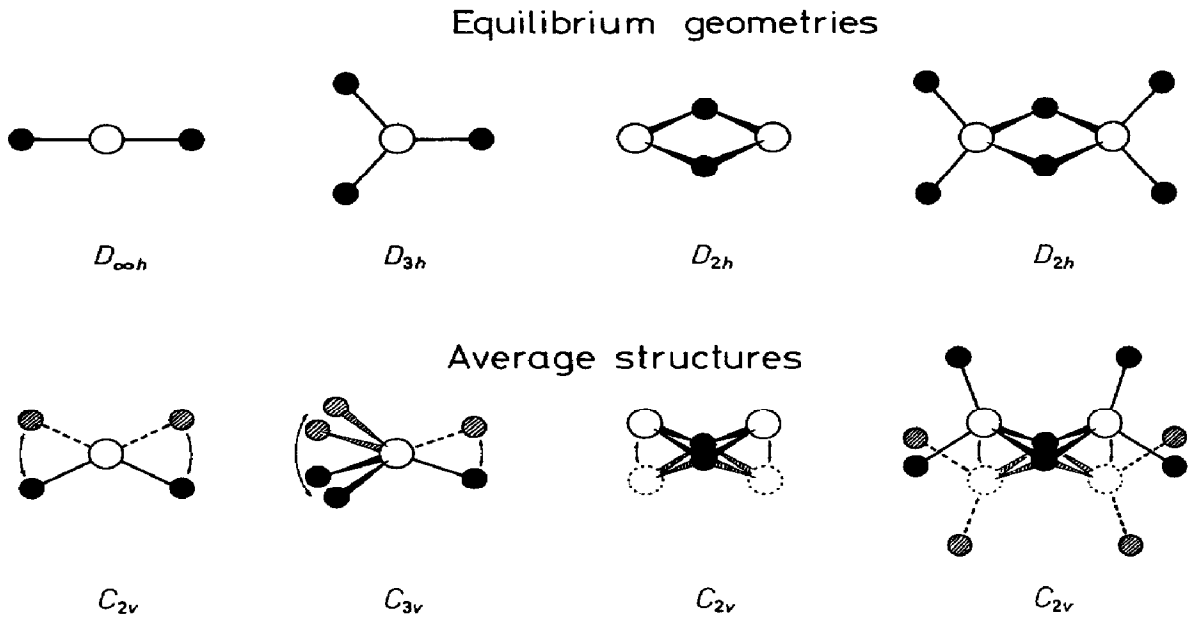

Fig. 2. Equilibrium and average structures for some high temperature metal halide molecular species.

possibility for investigating metal halide molecules. This is especially so because the information they provide for the same molecule is truly complementary.

The combination of mass spectrometry, IR and/or Raman, gas-phase and/or matrix isolation spectroscopy, can be a powerful approach. It may greatly facilitate the determination of the molecular types present in the vapor, their symmetry and, through correct assignment of their frequencies, the calculation of accurate thermodynamic data.

For geometry determination the combination of theoretical calculations, spectroscopic methods, and of the coupled electron diffraction–mass spectrometric technique can be suggested.

For high temperature electron diffraction the coupled electron diffraction–quadrupole mass spectrometric technique is a way to ensure the control and optimization of the vapor composition [19]. The purity of the sample and the suitability of the container can be checked, and the experimental conditions can be optimized this way before running the diffraction experiments.

Theoretical calculations can be performed to determine certain geometrical features which are not easily accessible by electron diffraction alone. An example would be the calculation of the difference between the dimer terminal and bridging bond lengths for MX_2 dihalides, with a certain amount of dimers in their vapor. Although the calculation may not be

reliable enough to provide the absolute value for the distances, their differences can be reliably determined. Then these differences can be used as constraints in the electron diffraction analysis.

Available frequencies from spectroscopy can be used to help determine the molecular shape. Spiridonov and coworkers [20], for instance, use a program for linear triatomic molecules in which a simultaneous refinement of electron diffraction and spectroscopic data produces geometrical parameters as well as force constants and vibrational parameters. Unfortunately, this approach can be used only in cases when no appreciable amount of dimers or other species contribute to the electron diffraction patterns.

The presence of different species in the vapor, as a rule, has not been considered in early electron diffraction studies. This is why, for example, the bond lengths determined for alkali halides differed so much from the microwave results (see ref. 21 for details). The electron diffraction values were indeed the mean of the bond lengths of the monomeric and dimeric species, both present in the vapor under the electron diffraction experimental conditions. The complexity of vapor composition is sometimes ignored even today. As was shown for MX_2 dihalides [15], for each per cent of ignored dimer presence, the bond length of the monomer refines to a value 0.1% higher than the bond length determined with proper considerations for dimer presence. The shift is always in the same direction, i.e. ignoring the dimers increases the apparent monomer bond distance.

B. MONOHALIDES

(i) Alkali halides

This is one of the most extensively studied areas in metal halide chemistry. Reference 22, for example, covers a wide range of topics from thermodynamics to theoretical calculations etc. Practical as well as theoretical importance motivate intensive research in this field. Questions of bonding theory, and in particular the extent of ionic and covalent bonding, and questions about the transition process from ionic crystals to gas-phase molecules are just two of the many intriguing groups of problems under investigation.

Gases of alkali halides contain predominantly monomeric molecules. Their geometry was determined by microwave spectroscopy with high accuracy. The parameters are collected in Table 1.

Perhaps it is worth mentioning that the geometry of alkali halides was first investigated by electron diffraction during the thirties in the pioneering days of this technique [28]. As simple diatomic molecules, they were thought to be among the simplest possible objects. It was only during the fifties that

TABLE 1

Bond lengths (Å) in alkali halides

MX	Monomer			Dimer	Crystal [a]
	MW [b]	ED [c]	ED	ED	XR [g]
	r_e	r_e	r_a	r_a	
LiF	1.5639			1.740(15) [f]	2.009
LiCl	2.0207				2.566
LiBr	2.1704				2.747
LiI	2.3919				3.025
NaF	1.9260				2.307
NaCl	2.3609	2.359(8) [d]	2.388(8) [d]	2.584(34) [d]	2.814
NaBr	2.5020	2.507(11) [e]	2.537(12) [e]	2.740(34) [e]	2.981
NaI	2.7114				3.231
KF	2.1716				2.664
KCl	2.6668	2.669(8) [d]	2.703(8) [d]	2.950(54) [d]	3.139
KBr	2.8208	2.829(8) [e]	2.865(4) [e]	3.202(22) [e]	3.293
KI	3.0478				3.526
RbF	2.2704				2.815
RbCl	2.7869	2.784(4) [d]	2.817(4) [d]	3.008(22) [d]	3.285
RbBr	2.9447	2.939(2) [e]	2.974(3) [e]	3.181(30) [e]	3.434
RbI	3.1768				3.663
CsF	2.3455				3.005
CsCl	2.9064	2.908(12) [d]	2.940(12) [d]	3.017(32) [d]	3.560
CsBr	3.0722	3.065(4) [e]	3.099(4) [e]	3.356(28) [e]	3.713
CsI	3.3152				3.950

[a] All crystals have the NaCl-type crystal structure except CsCl, CsBr and CsI, which have the CsCl-type lattice.

[b] MW, microwave spectroscopy. Ref. 23. [c] ED, electron diffraction. [d] Ref. 25. [e] Ref. 26. [f] Ref. 24. [g] XR, X-ray crystallography. Ref. 27.

the complexity of the vapors of alkali halides was discovered by different techniques, mainly by mass spectrometry (for references see ref. 21). Beside the monomers there is a considerable amount of dimers in the vapor. Higher associates are also present but in much smaller amounts.

The bond lengths of the monomeric molecules from up-to-date electron diffraction studies are also given in Table 1. In these studies the complexity of the vapor composition has been taken into account. The bond distances from the microwave studies are r_e parameters, while the electron diffraction values are r_a parameters. The r_e parameters refer to the equilibrium structure corresponding to the minimum position of the potential energy function. The r_a parameter is close to the thermal average distance at the temperature of the experiment. The latter, converted to r_e values, compare well with the microwave results. Most of the bond lengths in this review will

be quoted, however, as r_g parameter which is the thermal average length of a bond and thus has a well-defined and useful physical meaning.

Numerous methods have been used to calculate the bond distance in alkali halides; these were discussed elsewhere [22,25].

The alkali halide dimers have a planar rhombic structure with D_{2h} symmetry. Both electron diffraction [24–26] and IR spectroscopic [29] data are compatible with a four-membered ring structure. The possibility of a chain structure with alternating alkaline and halogen atoms has been ruled out. Theoretical calculations also find the rhombic structure more stable than the linear chain [30–32].

The bond distances experimentally determined for the dimers are given in Table 1. Their uncertainty is about one order of magnitude larger than usually given for bond distances. Both experimental and interpretational difficulties are responsible for this, among them the small relative amount of the dimers in the vapor and the correlation of the dimer and monomer parameters. The four-membered rings are supposed to be planar, but they always appear puckered under the electron diffraction experimental conditions in accordance with the low frequency b_{3u} normal modes of these molecules [29]. Leaving such a possibility out of consideration certainly influences the determination of the bond angles and through them, perhaps via correlation, even the determination of the M–X distances in the dimer. Table 1 includes the interionic distances in alkali halides in their crystals for comparison. In Fig. 3 also these data are compared for the chlorides, bromides and iodides. Inspection of these results shows that while the variation in bond lengths in the monomer molecules and in the interionic distances in the crystal follows the same trend, the dimer bond distances are rather scattered. Let us note here that the crystal structure of the three cesium halides is different from the others, i.e. eight coordination vs. six coordination, and the increase in the cesium–halogen distances is consistent with the increasing coordination number.

Even with the large uncertainties, the bond distances in the dimers all fall between the values in the respective monomers and crystals. Their bond angle variation follows the expected trend as shown in Table 2. For the same halogen, the X–M–X angle of the dimer decreases as the size of the alkali metal M increases. Different theoretical calculations predict the same trend (for references see, for example, ref. 25).

A matrix isolation IR spectroscopic study of highly concentrated alkali halide vapors indicated the presence of both trimeric and tetrameric species beside the monomers and dimers [29]. The hexagonal ring structure with D_{3h} symmetry was favored for the M_3X_3 trimers. Theoretical calculations using the polarizable ion model also favored this geometry [33,34]. According to ref. 34 the six-membered ring is one of the most stable building blocks in

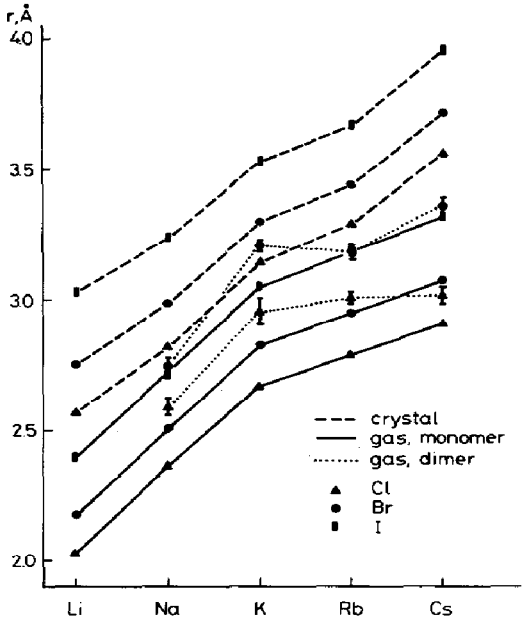

Fig. 3. Bond length variation in alkali halides.

ionic clusters. The linear chain was also found to be a stable configuration with lower binding energy but the rectangular planar trimer is unstable and opens up to yield a hexagonal ring (**1**).

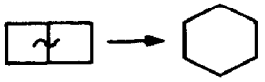

(**1**)

The electron diffraction investigation of lithium fluoride [24] detected the presence of about 10% of trimeric species in the vapor, but their geometry could not be determined. The assumption of a hexagonal ring structure for the molecule was consistent with the experimental data.

The lowest energy configuration for the M_4X_4 tetramers is the cube with

TABLE 2

X–M–X bond angles (deg) in alkali halide dimers

M_2X_2	Cl [25]	Br [26]
Na	101.4(24)	101.6(18)
K	96.0(24)	95.8(14)
Rb	88.2(20)	94.7(18)
Cs	83.6(13)	85.0(18)

TABLE 3

Bond lengths (Å) of Group 13 and transition metal monohalides [23]

MX	F	Cl	Br	I
Al	1.6544	2.1301	2.2948	2.5371
Ga	1.7744	2.2017	2.3525	2.5747
In	1.9854	2.4012	2.5432	2.7539
Tl	2.0844	2.4848	2.6181	2.8135
Cu	1.7449	2.0512	2.1734	2.3383
Ag	1.9830	2.2808	2.3931	2.5446

T_d or slightly distorted tetrahedral symmetry [33,34]. The assignment of the IR spectra, although very approximate, agrees with this. The next stable model with somewhat smaller binding energy is an eight-membered ring.

(ii) Group 13 monohalides

The stability of lower oxidation states among Group 13 metals increases in the sequence Al < Ga < In < Tl [35]. The bond lengths of all monohalides have been determined by microwave spectroscopy and are collected in Table 3. Indium halides with different valence states have been investigated by laser-Raman spectroscopy in the gas phase [36]. The spectra of InX vapors (X = Cl, Br) are characteristic of diatomic molecules. The InX_3 vapors are found to have a dimer–monomer In_2X_6–InX_3 equilibrium. The comparison of the melt and vapor spectra of the InX_2 species is also of interest. The presence of tetrahedral InX_4^- species in the melt suggests the mixed-valence structure, $In^{I}In^{III}X_4$. The predominant species of the vapor, however, are InX(g) and InX_3(g) monomeric molecules. The presence of a small amount of $InInX_4$ molecules in the vapor was not ruled out. The electron diffraction investigation of the vapors of InI_2 [37] resulted in similar results with an approximate vapor composition of $InI_3 : InI_2 : InI \approx 60\% : 30\% : 10\%$. For the In_2I_4 species, several models have been tested and the one resembling the mixed-valence condensed-phase structure was found to be the best (Fig. 4), with a considerably distorted InI_4 tetrahedron. Because of the very complicated vapor composition and the crude approximations that had to be used in the analysis, the geometrical parameters are not cited here.

Thallium(I) is the most stable oxidation state for the halides of this element. Thallous fluoride has been extensively studied (cf. ref. 2 (g)). According to mass spectrometric and vapor pressure measurements [38,39] dimeric species prevail in its vapor. Thallous halides have also been subject of vibrational [40] and photoelectron [41] spectroscopic studies. Three possi-

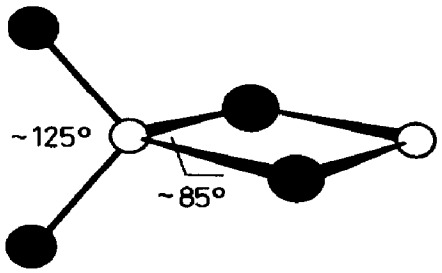

Fig. 4. Molecular model of the gas-phase In_2I_4 molecule.

ble models displayed in Fig. 5 have been considered and a linear geometry was supposed.

A low energy electron scattering experiment [42] indicated a considerable instantaneous dipole moment for Tl_2F_2 which cannot be explained by a symmetrical rigid linear or rhombic structure. Molecular beam deflection [43], however, was consistent with a non-polar dimeric structure of high symmetry. Both the linear and the planar rhombic models are consistent with this observation.

The electron diffraction data on thallous fluoride dimer may be interpreted by a rhombic structure and the linear model could be ruled out [44]. The geometrical parameters are r_g(Tl–F) 2.29(2) Å, r_g(Tl · · · Tl) 3.68(1) Å, r_g(F · · · F) 2.61(18) Å. The dimer content was around 80%.

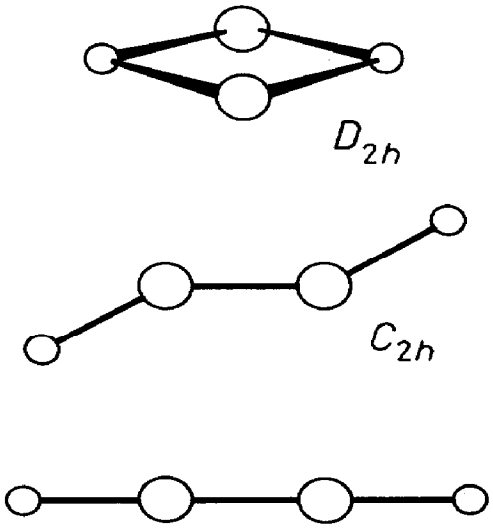

Fig. 5. The rhombic structure of Tl_2F_2. Other seriously considered models are also presented.

The molecule was assumed to have a planar four-membered ring with D_{2h} symmetry. An F–Tl–F angle of 73(2)° is calculated for the planar model from the measured Tl–F and Tl · · · Tl distances. This is consistent with the results from molecular beam deflection [43] and also with the IR and Raman spectra of matrix-isolated thallous fluoride [45]. The electron diffraction data, however, indicate a puckered ring (**2**) with C_{2v} symmetry for the

(**2**)

thermal average structure of the dimer. A puckering angle of about 17° can be calculated from the measured distances. A 34° out-of-plane bending vibrational amplitude for the Tl–F–Tl unit around the Tl · · · Tl axis corresponds to such puckering. This is in agreement with the large amplitude of 31° calculated for the out-of-plane bending coordinate [45] at the temperature of the experiment. The measured out-of-plane bending mode is 81 cm^{-1} [45], indicating great flexibility of the ring. The large instantaneous dipole moment [42] can be understood in view of this low frequency puckering. Since the interaction time of the electron beam and the molecules is very short, "frozen" nuclear configurations are detected by the low energy electron scattering experiment. Lesiecki and Nibler [45] commented upon the possible bending of the linear $D_{\infty h}$ symmetry structure to account for the large dipole moments. The π_u bending mode in the spectral assignment [40] for a linear structure yields a bending amplitude of about 2°, which gives a dipole of 0.8 D only [45]. A planar rhombic model with a 31° bending amplitude gives a dipole moment of 3.7 D, in agreement with the experimental data [42].

The geometry of Tl_2F_2 dimers thus seems to be well understood; it is planar rhombic with alternating Tl and F atoms. This four-membered ring, however, undergoes large-amplitude out-of-plane deformation motion at high temperatures.

(iii) Transition metal monohalides

The bond distances in cuprous and silver(I) halides from microwave spectroscopy are given in Table 3. The principal components of the vapor in equilibrium with solid cuprous chloride are trimers and tetramers according to mass spectrometric studies [46] and vapor pressure measurements [47]. Trimers were found to be the main component for cuprous bromide and iodide [47,48]. Monomers could be produced only by a double-oven technique in the matrix isolation IR spectroscopic study of CuCl and CuBr [49]. According to this study the vapors of AgCl and AgBr contain comparable

TABLE 4

Geometrical parameters of cuprous halide trimers

	Cuprous chloride			Cuprous iodide	
	Ref. 50	Ref. 51		Ref. 52	
T (K)	723	693	1333	693	
r_g (Cu–X)$_{mean}$(Å)	2.160(15) [a]	2.155(5)	2.179(5)	2.447(5)	2.447(5)
∠Cu–X–Cu (deg) [b]	~90	75–85	75–85	106(1)	108(1)
∠X–Cu–X (deg) [b]	~150	155–165	155–165	125(1)	127(2)
Polymeric species considered	Trimer	70%–90% trimer 10%–30% tetramer	60%–70% trimer Small amounts of monomers, dimers and tetramers	Trimer	Trimer
Configuration	Planar (supposed)	Different non-planar		Chair	Boat

[a] r_a. [b] Angles of the trimer.

amounts of monomers, dimers and trimers. All the dimer spectra are consistent with a rhombic structure, similar to that of the alkali halide dimers.

The trimers have a planar six-membered ring equilibrium structure with D_{3h} symmetry. The electron diffraction studies of cuprous chloride [50,51] and cuprous iodide [52] are consistent with this shape. The thermal average structures, directly determined from electron diffraction, are of lesser symmetry. There is a disagreement, however, between the spectroscopic and electron diffraction results regarding the atomic positions in the ring. The spectroscopic study reported a distorted six-membered ring with the metal atoms farther from the ring center than the halogen atoms [49], while the electron diffraction data were interpreted by an opposite arrangement. This is shown by the bond angles in Table 4. The electron diffraction reinvestigation of cuprous chloride vapor [51] illustrates the limitations of high temperature electron diffraction, caused mainly by the complicated vapor composition and the "floppiness" of the molecules undergoing large-amplitude deformation vibrations. The lowest possible temperature was 693 K where diffraction photographs could be recorded and even for this temperature the mass spectra indicated the presence of both trimeric and tetrameric species. Their relative abundance was about 80% trimers and 20% tetramers according to the electron diffraction analysis. The tetrameric species hindered the determination of the trimer structure without making the determination of the tetramer structure possible. The bond distances could not be distinguished and only a mean Cu–Cl distance was determined. The large

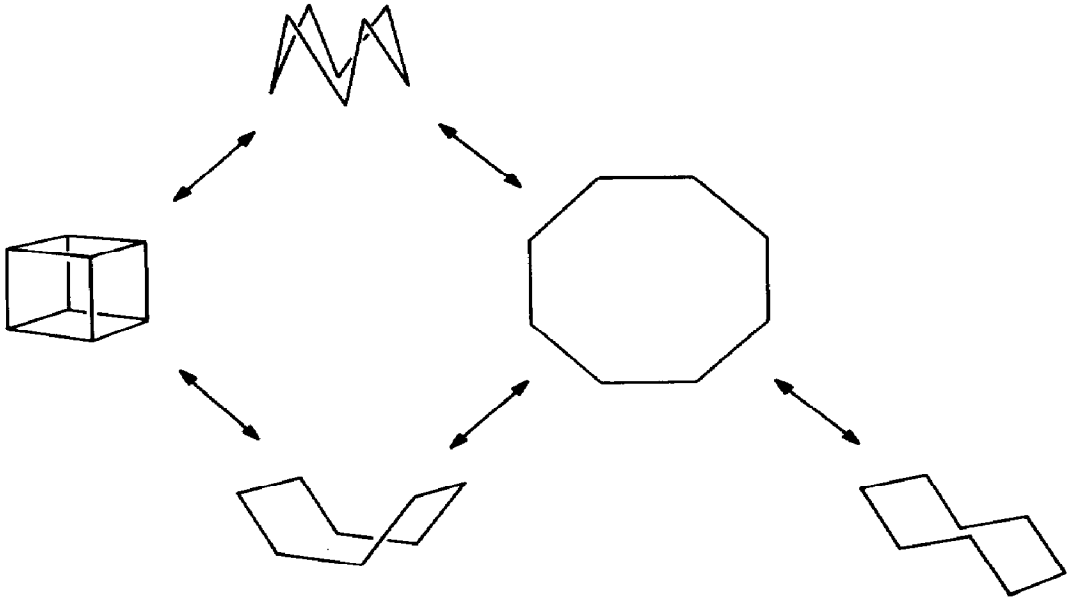

Fig. 6. Interrelation of different possible geometries for $(MX)_4$ tetramers.

number of a priori possible shapes for both oligomers presented additional problems. The experiment has been repeated at a considerably higher temperature of 1333 K in the hope of eliminating the tetrameric species. This did not happen, however. The vapor composition in this experiment was even more complicated than the one at the lower temperature, and the only parameter that could be reliably determined was again the mean Cu–Cl distance [51].

The electron diffraction results [51] agree with the spectroscopic results [49] in finding the eight-membered ring structure rather than the cube more favorable for the tetramer. This is in contrast with the results on alkali halide clusters [34], according to which the cube is the energetically most favorable model. The cube as a rigid model could be ruled out by the electron diffraction study of CuCl. However, many different lower symmetry ring forms were consistent with the electron diffraction data. As is seen in Fig. 6, the boat form and even the crown form of the tetramer can also be perceived as a distorted cube.

C. DIHALIDES

(i) Group 2 dihalides

According to mass spectrometric studies [53,54] the vapors of all Group 2 dihalides contain mainly monomeric MX_2 molecules.

TABLE 5

Bond angles (deg) of alkaline earth dihalides [a]

MX_2	F		Cl		Br		I	
	Exp.	Calc.	Exp.	Calc.	Exp.	Calc.	Exp.	Calc.
Be	180 [61]	180 [58]		180 [58]		180 [58]		180 [58]
Mg	180 [55, 57]	180 [58]	180 [56,57, 67]	180 [58]	180 [57]	180 [58]	180 [57]	180 [58]
Ca	140 [64]	133 [58]	180 [63,65, 67]	180 [58]	180 [63, 65]	180 [58, 62]	180 [65]	180 [58, 62]
	155 [61]	145 [62]		173 [62]				
Sr	108 [64]	115 [58]	120 [67]	143 [58]	180 [63]	164 [58]	180 [63, 66]	180 [58]
	135 [61]	127 [62]	142(8) [59]	133 [62]		133 [62]		161 [62]
Ba	100 [64]	103 [58]	100 [67]	125 [58]		138 [58]	148.0(9) [60]	154 [58]
	115 [61]	109 [62]	127(8) [59]	103 [62]		95 [62]		102 [62]

[a] References are given in square brackets after the bond angles.

The most intriguing question about their geometry is whether these molecules are linear or bent. There is a general agreement that the beryllium and magnesium dihalides are linear [1,55–58]. Similar consensus has been reached about the bent shape of all barium dihalides [1,58–64]. CaF_2 is bent and all the other calcium dihalides are linear [1,58,61,63–65]. SrF_2 and $SrCl_2$ are bent and SrI_2 is most probably linear [58,59,61,63,64,66,67]. $SrBr_2$ has not been studied much; molecular beam deflection measurements predict it to be linear [63], whereas according to theoretical calculations [58,62] it is bent. The bond angles of alkaline earth dihalides are collected in Table 5.

Electron diffraction is not very suitable for determining the shape of such molecules, since even linear metal dihalide molecules appear to be bent in the structure analysis owing to the large-amplitude vibrations of the molecule. This is practically the only method, however, for the determination of the bond length in these species.

The first electron diffraction studies of all Group 2 dihalides were reported in the fifties by the Moscow laboratory [68]. Since then several of them have been reinvestigated. The agreement between old and new results is good in some cases, whereas the differences in bond lengths are well outside the error limits in others. Already the early results established the expected trends in bond length variations and have been used for various empirical relationships [69]. The bond lengths from later studies are collected in Table 6. The available vibrational frequencies are compiled in ref. 70. From among the three normal modes the ν_2 bending mode of metal

TABLE 6

Bond lengths r_g (Å) in alkaline earth dihalides [a]

MX_2	F	Cl	Br	I
Mg	1.771(10) [55]	2.186(11) [56]		
Ca		2.483(6) [65]	2.616(7) [65]	2.830(7) [65]
Sr		2.616(6) [59] [b]		3.009(15) [66]
Ba		2.768(9) [59] [b]		3.150(4) [60]

[a] References are given in square brackets. [b] Here the errors were increased for consistency as we supposed that the original work quoted only least-squares standard deviations.

dihalides often falls below 100 cm^{-1} and is therefore rather difficult to determine experimentally. These frequencies, however, can sometimes be estimated from the electron diffraction data.

Some dimers have also been detected for these compounds by mass spectrometry [53,54,71]. This amounted to several per cent for the magnesium dihalides and decreased towards the barium dihalides. The dimers are assumed to have a planar, halogen-bridged geometry with D_{2h} symmetry (Fig. 7). Several of the fundamentals detected by the matrix isolation IR spectroscopic study of the magnesium dihalides were assigned to these Mg_2X_4 species [57]. Unfortunately, their presence was ignored in the electron diffraction structure analyses [55,56]. For the calcium dihalides a few per cent of dimers were found in the vapor by the electron diffraction–quadrupole mass spectrometric investigation [65] in accordance with the separate mass spectrometric studies [54,71].

Structural variations in Group 2 dihalides can be understood by supposing ionic bonding. Several empirical relationships were communicated [69,72], correlating geometrical and spectroscopic features involving polarizabilities and ionic radii. The Rittner polarizable ion model was used to calculate the equilibrium bond angles in ref. 58. Although the Rittner model was shown [72] to be sensitive to the values of metal ion polarizabilities and internuclear distances, and has limitations for quantitative predictions, the calculated values agree surprisingly well with the experimental results, thus supporting the assumption of ionic bonding in these molecules. The valence shell electron pair repulsion (VSEPR) model [73], however, predicts linear shapes for all these molecules. Simple Walsh diagrams [74] and semiempirical

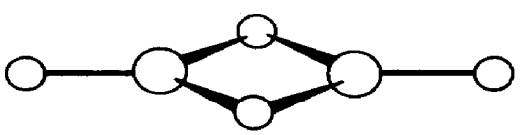

Fig. 7. Geometry of $(MX_2)_2$ dimers.

	F	Cl	Br	I
Be	l	l	l	l
Mg	l	l	l	l
Ca	b	l	l	l
Sr	b	b	(l)	l
Ba	b	b	b	b

l linear
b bent
( ) uncertain

Fig. 8. Shapes of alkaline earth dihalides.

calculations with only *s–p* basis sets [62] give the same results. A modified Walsh diagram [75], including *d* orbitals on the metal atom, accounts for the bent geometries of some alkaline earth dihalides. Semiempirical [62] as well as ab initio calculations [76] show the low lying metal orbitals essential in the bonding of these molecules. Their shape is then determined by the extent of metal *d*-orbital participation. The results of CNDO calculations [62] follow the general trend in the variation of bond angles; however, the actual values proved sensitive to the *d*-orbital exponents used in the calculation.

Returning to the ionic model of MX_2 dihalides, a bent geometry is favored by large, more polarizable metal ions and small, more electronegative halide ions [72]. Accordingly, the bond angle decreases in the following order: $MgF_2 > CaF_2 > SrF_2 > BaF_2$. For the bent barium halides, the bond angles are predicted to decrease with increasing electronegativity and decreasing size of the ligand: $BaI_2 > BaBr_2 > BaCl_2 > BaF_2$. The polarizable ion model calculations follow this trend and the predictions agree with available experimental data within experimental error. The variations in shape of alkaline earth dihalides are summarized in Fig. 8.

(ii) Group 12 dihalides

Only half of the possible dihalides of this group have been investigated by modern electron diffraction. No dimeric species were recorded in the combined electron diffraction–quadrupole mass spectrometric study of the zinc dihalides (X = Cl, Br, I) [77]. This is in agreement with a separate mass spectrometric study of ZnI_2 [78] according to which the vapor pressure of Zn_2I_4 species is about three orders of magnitude smaller than that of the monomers in the vapors of ZnI_2. The dimer content has not been checked in the other studies. The bond distances of the monomeric MX_2 molecules are

TABLE 7

Bond lengths in Group 12 dihalides

	r_g (Å)	Reference
ZnF_2	1.742(4)	79
$ZnCl_2$	2.062(4)	77
$ZnBr_2$	2.204(5)	77
ZnI_2	2.401(5)	77
$CdBr_2$	2.394(2)	80
$HgCl_2$	2.252(5)	81
HgI_2	2.568(4)	82

given in Table 7. All molecules were assigned linear geometries from electron diffraction.

The spectroscopic studies [83–86] are inconclusive for the shape of zinc and cadmium dihalides and have been interpreted in terms of a bent geometry for several mercury dihalides. Molecular beam deflection studies, however, indicate linearity for both zinc and mercury dihalides [87].

Let us consider now the geometry of zinc dihalides in some detail. The apparent bond angles of about 165° from electron diffraction would seem to be in good agreement with the 148°–180° angle intervals given by Givan and Loewenschuss [86] on the basis of the Raman spectra. The authors, however, stressed that the geometry was not outside the acceptable range of parameters for these molecules. At the same time the electron diffraction results must be considered in conjunction with the spectroscopic data, especially with the bending vibrational frequencies. Supposing linearity for the molecules, their ν_2 bending frequencies were estimated from electron diffraction [77].

A simple polarizability model was used by Drake and Rosenblatt [72] to account for the molecular shapes. Linear geometry was predicted for Group 12 dihalides using this model [72] and involving atomic rather than ionic polarizabilities. Although these are somewhat ionic systems, the extent of ionic bonding and the polarizability of the central atoms with partial charge transfer are not known.

(iii) Transition metal dihalides

The polarizability model predicts all first-row transition metal difluorides and dichlorides to be linear except for the difluorides of scandium, titanium and vanadium which are predicted to be bent [72]. The few ab initio calculations that have been carried out on these molecules resulted in linear configurations (ZnF_2 [88], CuF_2 [89], $MnCl_2$ [90], $CuCl_2$ [91]). The low lying *d* orbitals of the metals make predictions for these geometries difficult.

The available experimental data about the shape of these molecules are rather confusing. Here again the two most important tools for the determination of shape and symmetry are molecular beam deflection measurements and vibrational spectroscopy. Molecular beam deflection studies [87] indicated linear geometry for the first-row transition metal difluorides from manganese on. Spectroscopic studies agree on the non-linearity of TiF_2 [92,93]. The other difluorides are interpreted as linear or nearly linear from isotopic shift measurements [92,93]. The dichlorides were found to be linear in a series of spectroscopic studies [9,92,94], while a bent geometry for the iron, cobalt and nickel dichlorides was reported [95]. $CuCl_2$ was interpreted as bent by a gas-phase IR spectroscopic study [2 (f)]. Attempts to produce the latter species in an electron diffraction experiment in our laboratory have proved to be unsuccessful [96].

The difluorides of first-row transition metals from chromium to copper were investigated by electron diffraction and were all found to be linear [79,97,98]. The same is true for the dichlorides and dibromides of manganese, iron, cobalt and nickel [99–106]. The shape of the iron, cobalt and nickel dichlorides deserves a comment in the light of the above-mentioned matrix isolation IR spectroscopic study suggesting a bent geometry [95]. The controversy has been clarified in ref. 101 involving an analysis of the calculated and measured vibrational amplitudes. The linearity of the equilibrium geometries of $FeCl_2$ and other molecules in the series is well established.

In addition to monomers and dimers, higher associates have also been found by mass spectrometry in the vapors of chromium dichloride [107 (a)]. However, its electron diffraction analysis was carried out under the assumption of having only $CrCl_2$ and Cr_2Cl_4 species [108 (a)]. We reported a bent monomeric geometry from this analysis. Matrix IR spectra of chromium dichloride were not consistent with a bent structure [9,92]. A re-analysis of the electron diffraction data [108 (b)] is under way allowing for the presence of trimeric species in which case evidence points to the linearity of $CrCl_2$. Our information on the geometry of VCl_2 molecules is similarly uncertain. In this case, decomposition of $VCl_2(s)$ into $VCl_3(g)$ takes place in the vapor, according to mass spectrometry [107 (b)]. The VCl_2 molecules may well be linear and not bent as was suggested by our analysis of electron diffraction data [108 (a)] assuming association but no decomposition. The complicated vapor compositions of chromium dichloride and vanadium dichloride apparently prevent the reliable determination of their molecular shape by electron diffraction alone. The bond distances in all these dihalides are collected in Table 8.

The first-row transition metal dihalides are good examples to illustrate the importance of direct vapor control for the electron diffraction experiments.

TABLE 8

Bond lengths, r_g, (Å) of first-row transition metal dihalides [a]

MX_2	F	Cl	Br
V		2.18(1) [108 (b)]	
Cr	1.789(4) [97]	2.18(2) [108 (b)]	
Mn	1.811(4) [98]	2.202(4) [100]	2.344(6) [104]
Fe	1.769(4) [98]	2.151(7) [101]	2.310(5) [102]
Co	1.754(3) [98]	2.113(5) [100]	2.241(5) [105]
Ni	1.729(4) [98]	2.056(4) [103]	2.212(5) [106]
Cu	1.713(12) [79]		

[a] References are given in square brackets.

In the earlier studies of the dihalides ($MnCl_2$ [99 (a)], $CoCl_2$ [99 (b)] and $NiBr_2$ [106]) there was no simultaneous vapor control and monomers were assumed to be present alone on the basis of independent mass spectrometric evidence [109]. These early studies are being repeated now employing our improved experimental techniques. Preliminary results [100] show that whereas the vapors of $MnCl_2$ do not contain any detectable amount of dimers, there is about 4% of dimers present in the vapor of $CoCl_2$. The consequences of ignoring a dimer content were discussed in detail elsewhere [15]. $CuCl_2$ could not be studied by electron diffraction [96] because of the decomposition of the sample during evaporation. The same problem was encountered in the study of CuF_2 [79], where about equal amounts of monofluorides and difluorides were found to be present in the vapor.

The geometry of the dimers could only be determined partially. They have a four-membered halogen-bridged structure similar to the alkaline earth dihalide dimers (Fig. 7). The ring puckering under the electron diffraction experimental conditions probably corresponds to D_{2h} equilibrium symmetry with a planar ring. The symmetry lowering is again the result of large-amplitude deformation vibrations.

The dimers have two different M–X distances, bridging and terminal, and the bridging bond is considerably longer, by about 0.15–0.20 Å, than the terminal. The terminal bond of the dimer and the bond of the monomer have similar lengths and it proved to be impossible to determine the difference.

Few dihalides other than first-row transition metal dihalides have been investigated in the gas phase. The difluorides and dichlorides of samarium, europium and ytterbium and UCl_2 were studied by spectroscopy and found to be bent [110–112]. On the basis of isotopic shifts the bond angle of $YbCl_2$ was estimated to be $126 \pm 5°$ [112]. The electron diffraction study of SmI_2 yielded a bond angle of 135(10)° and an r_e(Sm–I) distance of 2.944(7) Å

TABLE 9

Geometrical parameters of Group 14 dihalides

AX_2		F		Cl	Br	I
C	r (Å)	1.304 [a]	1.291 [b]	1.756 [b]		
	∠ (deg)	104.8	104.7	109.4		
Si	r (Å)	1.590 [c]		2.089(4) [d]	2.249(5) [d]	
	∠ (deg)	100.8		103.1(6)	102.9(3)	
Ge	r (Å)	1.732 [e]		2.186(4) [f]	2.337(13) [g]	
	∠ (deg)	97.2		100.4(4)	101.4(9)	
Sn	r (Å)			2.346(7) [h]	2.512(3) [i]	2.706(4) [i]
	∠ (deg)			99 (1)	100.0(7)	103.8(7)
Pb	r (Å)	2.033(3) [i]		2.445(5) [j]	2.597(3) [i]	2.804(4) [i]
	∠ (deg)	97.8(20)		97.6(15)	98.8(15)	99.7(8)

[a] Microwave spectroscopy (MW), r_o, [114]. [b] ab initio, r_e, [123]. [c] MW, r_e, [115]. [d] Electron diffraction (ED), r_g, [117]. [e] MW, r_e, [116]. [f] ED, r_g, [118]. [g] ED, r_g, [119]. [h] ED, r_a or r_g, [120]. [i] ED, r_g, [121]. [j] ED, r_g, [122].

[113]. The dihalides of all lanthanide and actinide elements are predicted to be bent by the polarizability model owing to their large polarizable central atom [72].

(iv) Group 14 dihalides

All Group 14 dihalides have unambiguously bent geometry, according to both experimental (vibrational spectroscopy (for references see ref. 70), microwave spectroscopy [114–116], electron diffraction [117–122]) and theoretical [123,124] studies. The geometrical parameters are presented in Table 9. The bent shape of these molecules is in agreement with the predictions of the VSEPR model [73]. The bond angles increase in the order F < Cl < Br < I with a given central atom, again in accordance with this model. Another trend is observed down the group; the angles decrease in the order C > Si > Ge > Sn > Pb with the same halides. Both variations can be interpreted with non-bonded interactions as well. An increasing ratio of ligand size to central atom size results in increased non-bonded interactions and larger bond angles.

No dimers have been detected in the electron diffraction studies of these molecules. The IR spectroscopic investigation of GeF_2 [125], however, suggested the presence of Ge_2F_4 dimers with C_{2h} symmetry (**3**). The stereo-

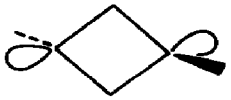

(**3**)

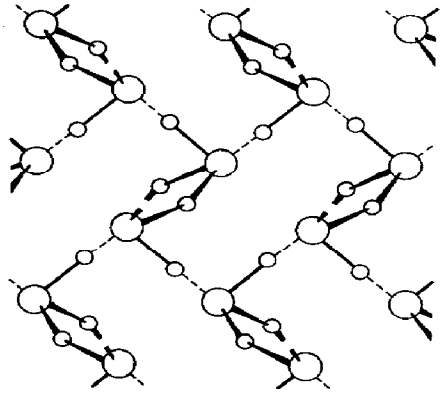

Fig. 9. Part of the GeF_2 crystal structure (after ref. 126).

chemical activity of the lone electron pairs is obvious even in the crystal phase as seen in the structure of the germanium difluoride crystal in Fig. 9. A UV photoelectron spectroscopic study of gaseous SnF_2 [127] reported the presence of both monomers and dimers, in accordance with mass spectrometric studies [128], but no direct geometry determination has appeared yet. The Sn_2F_4 dimer probably has the same geometry as Ge_2F_4. For comparison, tetrameric units build up the crystal of SnF_2 (Fig. 10), with a puckered eight-membered ring [129]. The angles around the Sn atom are smaller than 90° indicating stereochemical activity of the lone pair electrons.

(v) Group 16 dihalides

Of the Group 16 dihalides, the dihalides of selenium and tellurium should be mentioned here. They also have a bent geometry according to spectro-

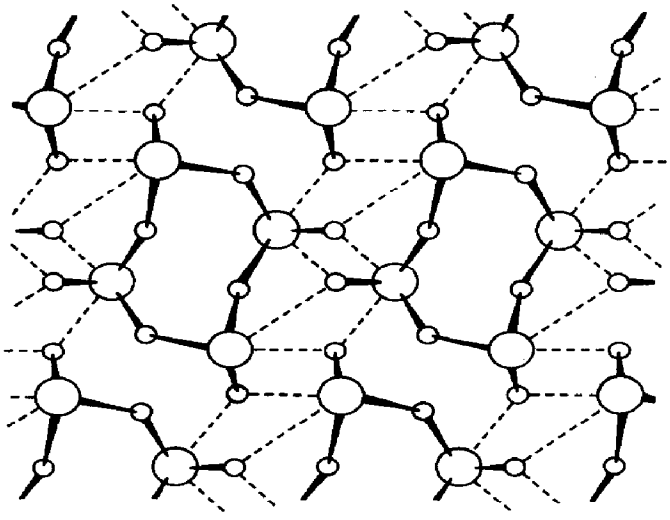

Fig. 10. Tetrameric units in the crystal of SnF_2 (after ref. 129).

scopic [130] and electron diffraction [131,132] studies, again in accordance with the VSEPR model. The geometrical parameters are r_a(Se–Cl) 2.157(3) Å, Cl–Se–Cl 99.6(5)°, and r_a(Te–Cl) 2.329(3) Å, Cl–Te–Cl 97.0(6)°. The variation in bond lengths and bond angles in the series OCl_2, SCl_2, $SeCl_2$ and $TeCl_2$ follows the same trend as in the dihalides of Group 14.

D. TRIHALIDES

(i) Group 13 halides

The trihalides of the Group 13 elements exist as monomers and dimers in the vapor phase [133,134]. The fluorides have relatively low volatility and their vapor consists predominantly of monomers [135]. Dimers are the only or predominant species of the vapors of $AlCl_3$, $AlBr_3$ and $GaCl_3$ at lower temperatures [133,134,136]. The mass spectra of $AlCl_3$ also indicated a small amount of trimeric species [134]. At higher temperatures only monomers are present.

(a) Monomers

They have a well-established planar shape with D_{3h} symmetry. References to spectroscopic studies prior to 1983 can be found in ref. 70. Some more recent studies have been made on $GaCl_3$ [137], $AlCl_3$ [138], and $AlBr_3$, AlI_3, and $GaCl_3$ [139]. A planar configuration is predicted for all these monomers by the polarizability model [72]. The bond lengths determined by electron diffraction are given in Table 10.

(b) Dimers

A geometrical model of M_2X_6 dimeric molecules is shown in Fig. 11. The

TABLE 10

Bond lengths in monomeric Group 13 trihalides

MX_3	T (K)	r_g(M–X) (Å)	Reference
AlF_3	1100	1.633(3)	140
		1.60 [a]	141
GaF_3	910	1.725(4)	140
$AlCl_3$	800	2.06(1)	142
	1150	2.068(4)	143
	1410	2.074(4)	143
		2.05 [a]	141
GaI_3	528	2.458(5)	144
InI_3	710	2.641(5)	145

[a] r_e, ab initio results.

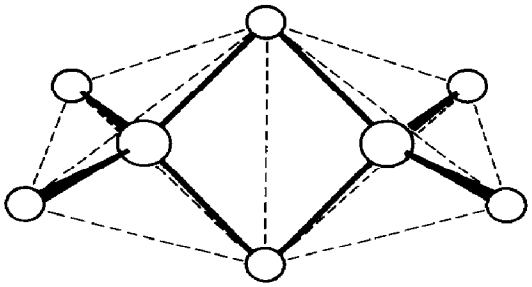

Fig. 11. Geometry of $(MX_3)_2$ dimers.

two monomeric units share two halogens (one from each) in a four-membered ring. The molecules can also be looked at as two tetrahedra sharing a common edge. The metal atoms are located at the centers of the tetrahedra and the halogen atoms at the apexes. The possibility of other arrangements with one or three halogen bridges was investigated and ruled out by ab initio calculations carried out for Al_2F_6 [141].

The symmetry of the M_2X_6 molecules is D_{2h} according to spectroscopic studies [138,139]. This implies a planar four-membered ring. The ring puckering mode of all these molecules, however, is calculated [139] to be smaller than 40 cm^{-1}, predicting very flexible rings. Such low frequencies have not yet been observed experimentally for these molecules. The M_2X_6 dimers appear to be puckered indeed under the electron diffracton experimental conditions [136]. This symmetry lowering, from D_{2h} to C_{2v}, is the consequence of low frequency, large-amplitude puckering motion of the molecule around the axis connecting the two bridging halogen atoms (**4**)

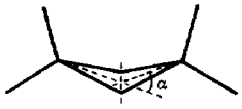

(**4**)

(see also Fig. 2). The geometrical parameters of the dimers are collected in Table 11, with the results of minimum basis ab initio calculations [141] included for comparison.

The bridging M–X bonds are considerably longer than the terminal ones. This is consistent with the spectroscopic results [139], according to which the stretching frequencies of the terminal bonds are about 2.4 times larger than those of the bridging bonds. There is a remarkable constancy in the differences and ratios of the lengths of these two bond types: the bridging bonds are about 0.19 Å longer than the terminal bonds and the ratio of the terminal bond to bridge bond is about 0.92. The X_b–M–X_b angle increases with increasing halogen bulkiness for the same metal.

TABLE 11

Geometrical parameters of dimeric Group 13 trihalides

M_2X_6	$r_g(M-X)_t$ (Å)	$r_g(M-X)_b$ (Å)	X_t-M-X_t (deg)	X_b-M-X_b (deg)	α [a] (deg)	Ref.
Al_2F_6	1.60 [b]	1.72 [b]	124.6 [b]	80.0 [b]		141
Al_2Cl_6	2.05 [b]	2.24 [b]	122.8 [b]	94.7 [b]		141
	2.066(2)	2.254(4)	123.5(16)	91.0(5)	23.4(60)	136
Al_2Br_6	2.223(5)	2.417(8)	122.8(33)	92.2(9)	23.3(140)	136
Al_2I_6	2.451(13)	2.637(29)	115.1(74)	99.5(45)	25.0 [c]	136
Ga_2Cl_6	2.100(2)	2.303(3)	124.7(18)	88.3(8)	20.5(33)	136
Ga_2Br_6	2.246(3)	2.449(9)	128.2(30)	91.1(22)	25.0 [c]	136

[a] Root-mean square amplitude of ring puckering. [b] r_e, ab initio calculation. [c] Assumed value.

Dimers have been found in the vapors over InI_3 [37]. The geometrical parameters are not cited here because of the many constraints used in the analysis.

(ii) Group 15 trihalides

These are all pyramidal molecules, as expected owing to the presence of the lone electron pair on their central atom. The geometrical parameters of the trihalides studied so far are collected in Table 12. The bond angles are all smaller than the ideal tetrahedral angle in accordance with the VSEPR theory [73]. Their variation can also be accounted for by this model. The

TABLE 12

Geometrical parameters of Group 15 trihalides

AX_3	$r_g(A-X)$ (Å)	∠X–A–X (deg)	Reference
AsF_3	1.710(3)	96.0(3) [a]	146
	1.706(2)	96.2(2)	147
$AsCl_3$	2.166(3)	98.6(4) [a]	146
$AsBr_3$ [b]	2.326(2)	99.6(1)	148
$AsBr_3$ [c]	2.329(2)	99.6(2)	148
AsI_3	2.557(5)	100.2(4)	144
$SbCl_3$	2.333(3)	97.2(10)	149 (a)
	2.334(4)	97.1(10)	149 (b)
$SbBr_3$	2.490(3)	98.2(6) [a]	151
SbI_3 [d]	2.719(5)	99.1(10)	152
$BiCl_3$	2.425(5)	97.3(2)	150

[a] $\angle_\alpha$ value. [b] At 373 K. [c] At 466 K. [d] Unidentified, possibly r_a.

XAX angle of the same central atom increases as the electronegativity of the ligands decreases. This variation can also be explained by non-bonded interactions, i.e. with increasing ratio of ligand size to central atom size the bond angles somewhat open out. As for the variations down the group, central atoms with diminishing electronegativity in the environment of the same ligands will have decreasing bond angles. For comparison, the bond angles of NCl_3 and PCl_3 are 107.8(4)° [153] and 100.3(1)° [154] respectively. All bond angle variations follow the same trends as those observed for the Group 14 dihalides.

(iii) Transition metal trihalides

Spectroscopic studies of transition metal (non-rare earth) trihalides are rather scarce and inconclusive. Molecular beam deflection studies indicate pyramidal geometry for ScF_3 [155] in agreement with an earlier electron diffraction study [156], while the matrix isolation IR results could be interpreted by a planar structure [157]. ESR results are in agreement with planar geometry for TiF_3, CrF_3 and FeF_3 [93]. However, the planarity of TiF_3 could not be concluded from its IR spectra [158]. ScF_3, VF_3, and CrF_3 were recently studied by electron diffraction [159]. The effective bond angle is around 116–117° in all these molecules. It was concluded, however, that the equilibrium structure is planar with D_{3h} symmetry with allowance for the shrinkage effect. The electron diffraction study of FeF_3 [160] resulted in a thermal average angle of 116.1(8)°, which could also be interpreted with a planar equilibrium structure if the frequency of the out-of-plane vibration is rather small. Lacking experimental vibrational data, however, electron diffraction alone cannot give a definitive answer. The bond lengths (r_g) of these molecules are as follows: ScF_3 1.847(2) Å, VF_3 1.751(3) Å, CrF_3 1.732(2) Å, FeF_3 1.763(4) Å.

Turning to the chlorides, a recent matrix isolation IR study of $CrCl_3$ confirms the planarity of this molecule [9]. $FeCl_3$ was found to be planar by IR [161] and pyramidal by a Raman spectroscopic study [162]. Although the electron diffraction study of iron trichloride at higher temperature could not yield accurate geometrical data [15] the thermal average bond angle of about 117° suggests that the equilibrium geometry should be planar. WCl_3 was investigated by electron diffraction [163] and a T-shaped C_{2v} symmetry structure was proposed by analogy with the structure of, for example, ClF_3 but this conclusion may well be incorrect. Whereas the stereochemical influence of the lone pairs of chlorine as central atom is a determining factor, this is not so obvious for a transition metal as central atom. Unfortunately the electron diffraction experiment on WCl_3, covering a very limited range of the scattering region, was not coupled with a mass spectro-

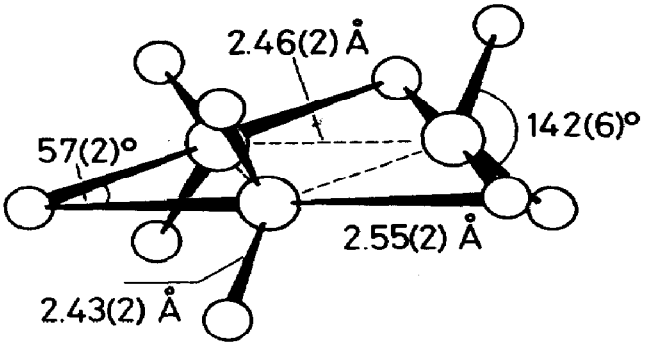

Fig. 12. Shape and geometrical parameters of the Re_3Br_9 molecule.

metric control of the vapor composition. A separate mass spectrometric study indicated the presence of dimers and trimers together with the monomers [164].

Iron trichloride behaves similarly to the Group 13 trihalides in its vapor composition as well as in its molecular geometry. At low temperatures the vapor of iron trichloride consists entirely of dimers. Its geometry is analogous to that of Al_2Cl_6 (see Fig. 11) and the geometrical parameters from its electron diffraction study [165] are as follows: $(Fe–Cl)_t$ 2.129(4) Å, $(Fe–Cl)_b$ 2.329(5) Å, $Cl_t–Fe–Cl_t$ 124.3(7)° $Cl_b–Fe–Cl_b$ 90.7(4)°, and α 16.7(10)°. The vapors of tungsten trichloride contain a considerable amount of dimers as well as trimers according to the mass spectra [164]. W_2Cl_6 was found [166] to have a similar geometry to that of Fe_2Cl_6. Its electron diffraction analysis suffered from the same difficulties as that of WCl_3 (see above).

Rhenium tribomide exists in a trimeric form in the vapor according to an electron diffraction study [167]. The molecular configuration and the main geometrical parameters are shown in Fig. 12. The short Re–Re distance, compared with the covalent radius of 1.283 Å [168], indicates a direct chemical bond between the rhenium atoms. Mass spectrometric studies of rhenium halide vapors and X-ray diffraction studies of crystalline rhenium halides [21] are also consistent with the presence of trimeric molecules. The resonance Raman spectra of matrix-isolated $ReCl_3$ vapors [169] were also interpreted with a hexagonal ring trimer of D_{3h} symmetry.

(iv) Lanthanide (rare earth) trihalides

The rare earth trihalides have been rather extensively studied. The two main questions about their structures are the molecular shape and the bond length variation.

While the monomeric Group 13 trihalides are all planar, experimental and theoretical evidence point to the non-planarity of the rare earth trihalides.

TABLE 13

Bond angles in rare earth trihalides

LnX_3	X–M–X (deg)	Reference
PrF_3	102.6(28)	159
GdF_3	108.4(24)	159
HoF_3	107.7(22)	159
$LaCl_3$	112.5(25)	174
$PrCl_3$	110.8(30)	175
$GdCl_3$	113.0(15)	176
$TbCl_3$	110.5(17)	177
$HoCl_3$	111.2(20)	175
$LuCl_3$	111.5(20)	156
$LaBr_3$	115.5(20)	178
$GdBr_3$	113.7(18)	179
$LuBr_3$	114.5(18)	179
PrI_3	112.7(22)	180
NdI_3	111.8(18)	180
GdI_3	108.0(20)	180
LuI_3	114.5(21)	180

Molecular beam deflection measurements [155] as well as IR spectroscopic studies [157,170,171] indicated pyramidal geometries for these molecules. In one case, however, the IR spectra were interpreted with planar geometry [172]. Calculations also predict C_{3v} symmetry for the trihalides of lanthanides [173]. Electron diffraction studies are in agreement with pyramidal geometry for these molecules. The bond angles and references are given in Table 13.

As has already been discussed, the apparent bond angle from electron diffraction may be smaller than 120°, even for a planar MX_3 molecule. If the molecule appears to be pyramidal even after applying the shrinkage corrections, it is an indication that the equilibrium symmetry is C_{3v}. The harmonic equilibrium bond angle of PrF_3, GdF_3 and HoF_3 was found to be 105.0(15)°, 109.0(23)° and 110.8(12)° respectively [159]. Although anharmonicity corrections were ignored in these corrections, these values are thought to be a good representation for the equilibrium structure.

According to the polarization model mentioned before [72], the large more polarizable central atoms are the prime origin for pyramidal geometry in contrast with the Group 13 trihalides which are planar with their smaller central atoms.

The bottom curve in Fig. 13 shows that the M^{3+} ionic radii gradually decrease going from lanthanum through the whole lanthanide series [35]. This is the well-known "lanthanide contraction", which is the consequence of the imperfect shielding of $4f$ electrons from the nucleus.

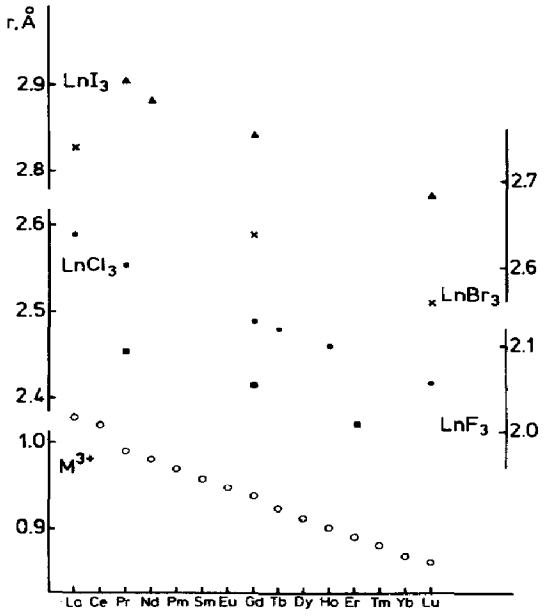

Fig. 13. Variations in ionic radii and bond lengths of rare earth trihalides.

Figure 13 also displays the bond lengths of lanthanide trihalides determined so far. Although their number is still small, it is seen that their variation closely follows the variation in the M^{3+} ionic radii. The differences between the metal–halogen distances and the ionic radii with their standard deviations are 1.107(6) Å, 1.577(4) Å, 1.703(4) Å and 1.906(6) Å for the fluorides, chlorides, bromides and iodides respectively. Using these differences, yet unknown bond lengths of other lanthanide trihalides can be estimated. They are given in Table 14 together with experimental data. Similar predictions based on fewer data appeared in ref. 181.

E. TETRAHALIDES

The vapor phase of tetravalent metal halides contains only monomeric molecules; no appreciable amount of polymeric species has been recorded.

(i) Tetrahedral tetrahalides

(a) Group 14 tetrahalides

These tetrahalides are the best examples of a regular tetrahedral arrangement. From among the Group 14 elements only germanium, tin and lead are considered here; geometrical parameters are available for $GeCl_4$ [182], $GeBr_4$ [183] and $SnCl_4$ [184], i.e. 2.113(3), 2.272 (3) and 2.281(4) Å respectively.

TABLE 14

Experimental (r_g, in italics) and estimated bond lengths (Å) of lanthanide trihalides

LnX_3	Fluorides	Chlorides	Bromides	Iodides
La	2.139(10)	*2.590(6)*	*2.741(5)*	2.938(10)
Ce	2.127(10)	2.577(10)	2.723(10)	2.926(10)
Pr	*2.091(3)*	*2.553(6)*	2.693(10)	*2.904(6)*
Nd	2.090(10)	2.540(10)	2.686(10)	*2.881(5)*
Pm	2.077(10)	2.527(10)	2.673(10)	2.876(10)
Sm	2.065(10)	2.515(10)	2.661(10)	2.864(10)
Eu	2.054(10)	2.504(10)	2.650(10)	2.853(10)
Gd	*2.053(3)*	*2.489(6)*	*2.640(10)*	*2.841(5)*
Tb	2.030(10)	*2.478(5)*	2.626(10)	2.829(10)
Dy	2.019(10)	2.469(10)	2.615(10)	2.818(10)
Ho	*2.007(3)*	*2.459(6)*	2.604(10)	2.807(10)
Er	1.997(10)	2.447(10)	2.593(10)	2.796(10)
Tm	1.987(10)	2.437(10)	2.583(10)	2.786(10)
Yb	1.975(10)	2.425(10)	2.571(10)	2.774(10)
Lu	1.968(10)	*2.417(6)*	*2.506(1)*	*2.771(6)*

(b) Transition metal tetrahalides

The titanium subgroup is one of the best-studied groups; in addition to many spectroscopic studies (for references see ref. 70), all the 12 tetrahalides have been investigated by electron diffraction. References to these works and the metal–halogen bond distances are collected in Table 15.

The ionic radii of zirconium and hafnium are practically identical [35] and their chemical behavior is similar as a result of the lanthanide contraction. The bond lengths of the corresponding zirconium and hafnium tetrahalides are the same within experimental error, except for the bromides where further contraction is observed.

From among the Group 5 elements, only the tetrahalides of vanadium have been studied so far. The bond lengths are VCl_4 2.138(2) Å [186] and VBr_4 2.276(4) Å [191]. The V–X bonds are shorter than the corresponding Ti–X bonds. This is in accordance with the generally observed contraction in a period.

TABLE 15

Bond lengths r_g (Å) of tetrahedral transition metal tetrahalides [a]

MX_4	F	Cl	Br	I
Ti	1.756(3) [185]	2.170(2) [186]	2.339(5) [187]	2.546(4) [187]
Zr	1.902(4) [188]	2.328(5) [189]	2.465(4) [187]	2.660(10) [187]
Hf	1.909(5) [188]	2.316(5) [190]	2.450(4) [187]	2.662(8) [187]

[a] References are given in square brackets.

The vanadium halides are interesting objects for structure determination, since they should be subject to Jahn–Teller distortions [192]. Both VCl_4 and VBr_4 are believed to be in a doubly degenerate ground electronic state in a tetrahedral configuration. The electronic and nuclear motions in the molecule are essentially mixed in such cases. The doubly degenerate deformation vibration, $\nu_2(E)$, should be strongly involved in vibronic interactions with the degenerate ground electronic state and they would cause a distortion of the molecules from the regular tetrahedral configuration. The electron diffraction results, however, do not show any deviation from the regular tetrahedral geometry within experimental error [186,191]. Different distorted models (D_{2d}, D_2, C_{2v}) have been tested in the structure analysis of VBr_4 but they all gave poorer agreement with experiment than the regular tetrahedral model. Thus there is no indication of a Jahn–Teller distortion. This absence of evidence, however, refers only to the so-called static Jahn–Teller effect. As was shown by Bersuker [193], the static Jahn–Teller effect can be observed only in the presence of external influence. Jahn–Teller distortions displayed by systems without any external influence are of a dynamic nature. There may be many minimum-energy distorted structures in such systems. Whether an experiment will or will not detect such a dynamic Jahn–Teller effect depends on the relationship between the time scale of the physical measurement used for the investigation and the mean lifetime of the distorted configurations.

Among the electron diffraction results, a marked increase in the mean amplitudes of vibration compared with the calculated ones is an indication of the possible presence of several distorted configurations. If this is the case, it is still only a thermal average that appears from the analysis.

The matrix isolation IR spectrum of $CrCl_4$ [9] and the electron diffraction data of $MoCl_4$ and $MoBr_4$ [194] are compatible with a regular tetrahedral structure. However, the results of the electron diffraction study of WCl_4 [195] were interpreted with a C_{2v} symmetry configuration, by analogy with the Group 16 tetrahalides (see next section and Fig. 14). The stereochemical role of the lone electron pair in a transition metal atom should be considered with caution (see also p. 62). Considering the fact that the regular tetrahedral model gave only slightly worse agreement with experiment than a trigonal bipyramid with a vacant equatorial position [195], the possibility that a slightly distorted tetrahedral model would also fit the electron diffraction data cannot be ruled out.

(ii) Non-tetrahedral tetrahalides

(a) Group 16 tetrahalides

These molecules have a C_{2v} symmetry structure corresponding to a

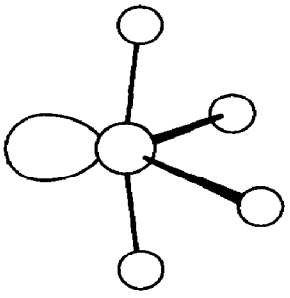

Fig. 14. The geometry of group 16 tetrahalides, with a lone electron pair on their central atom.

trigonal bipyramid with the lone electron pair of the central atom in an equatorial position (Fig. 14), in accordance with the VSEPR model.

All tetrahalides belonging to this group have such a geometry; only the selenium and tellurium halides are mentioned here. The C_{2v} symmetry was established for SeF_4, TeF_4 [196] and $TeCl_4$ [197] by vibrational spectroscopy. The geometrical parameters of SeF_4 from a microwave spectroscopy study [198] are $(Se-F)_{eq}$ 1.682(4) Å, $(Se-F)_{ax}$ 1.771(4) Å, $F_{eq}-Se-F_{eq}$ 100.55(70)° and $F_{ax}-Se-F_{ax}$ 169.20(70)°.

(b) Transition metal tetrahalides

Whereas the configuration of simple main group molecules can usually be predicted by simple theories, such as the VSEPR model, the structures of transition metal halides are generally not amenable to such simple predictions. Other empirical models, such as the polarizability model [72], may be more successful here. However, the ionicity of the bonding or the presence of partially filled *d* orbitals on the central atom seriously complicates matters and makes the prediction of molecular geometries difficult by simple empirical relationships.

TABLE 16

Bond lengths in trigonal bipyramidal monomeric pentahalides

MX_5	$r(M-X)_{eq}$ (Å)	$r(M-X)_{ax}$ (Å)	Reference
AsF_5	1.656(4)	1.711(5)	147
$SbCl_5$	2.277(5)	2.338(7)	204
VF_5	1.704(5)	1.732(7)	205
$NbCl_5$	2.241(4)	2.338(6)	206
$TaCl_5$	2.227(3)	2.369(4)	206
$TaBr_5$	2.412(4)	2.473(8)	207

Several lanthanide and actinide tetrahalides have been investigated so far and there is indication of some symmetry lowering from a regular tetrahedral geometry. Spectroscopic [199], mass spectrometric [200] and electron diffraction [201,202] data on different thorium and uranium tetrahalides were all interpreted in terms of a lower-than-tetrahedral symmetry. The most often suggested geometry is a model with C_{2v} symmetry, which is derived from the regular tetrahedron with opposite angular distortions. The electron diffraction investigation of CeF_4 [203] also suggested a distorted geometry with either C_{3v}, or D_{2d} or C_{2v} symmetry.

F. PENTAHALIDES

Pentahalides exist in the vapors in monomeric and different polymeric species. Fluorides appear very often as dimers or trimers in the vapor phase, while chlorides and bromides are more frequently found as monomers.

(i) Monomers

The Group 15 and Group 5 monomeric pentahalides all have a regular trigonal bipyramidal configuration. Vibrational frequencies are given in ref. 70, and the geometrical parameters are collected in Table 16. The axial bonds are longer than the equatorial according to expectation. Their differences are larger in the pentachlorides than in the pentafluorides: $NbCl_5$ [206], 0.097; $TaCl_5$ [206], 0.142; PCl_5 [208], 0.104; PF_5 [209], 0.043; AsF_5 [147], 0.055; VF_5 [205], 0.027 Å. This could be interpreted by weaker repulsions of the bonding pairs to fluorine owing to its greater electronegativity. The difference for $TaBr_5$ is again rather small, 0.061 Å. The mean bond distances in $NbCl_5$ and $TaCl_5$ are nearly identical as a consequence of the lanthanide contraction.

Although molecular beam deflection experiments [210] suggested some distortion of the regular trigonal bipyramidal arrangement for VF_5, the electron diffraction results were consistent with D_{3h} symmetry.

The possibility of Berry-type [211] permutational isomerism ("pseudorotation") was also investigated for VF_5. The diffraction picture did not indicate the presence of intermediate geometries that would occur along a supposed inversion coordinate. The barriers to "pseudorotation" for the niobium and tantalum halides were estimated from the electron diffraction data [206,207].

The Group 6 transition metals also have pentahalides. Since their electronic configuration is d^1, it is degenerate with the one electron occupying an e'' orbital in a supposed D_{3h} symmetry structure. Therefore these

molecules should be subject to Jahn–Teller distortion just as VCl_4 is in a tetrahedral configuration.

CrF_5 was found to have a lower, C_{2v}, symmetry geometry, rather than the more symmetric D_{3h} structure, in an electron diffraction study [212]. The average Cr–F bond length is 1.708(2) Å. The C_{2v} geometry is derived from the D_{3h} structure by opening one of the equatorial angles and then by bending the two axial bonds toward this widening angle (**5**). According to

(**5**)

Jacob et al. [212], the C_{2v} symmetry structure of CrF_5 may be the result of averaging over different distorted structures owing to the dynamic Jahn–Teller effect.

In connection with the above investigation, it is interesting to mention that a recent matrix isolation IR study of CrF_5 [213] failed to detect the pentafluoride in the vapor; according to the authors the vaporization of solid CrF_5 yielded CrF_4 and CrF_6 by disproportionation.

$MoCl_5$ and WCl_5 are also monomeric, at least predominantly, in the gas phase. According to their electron diffraction study [214,215] they have D_{3h} symmetry as the effective configuration at the electron diffraction experimental temperature. Nevertheless, there is a possibility that the equilibrium configuration is actually C_{4v} with a low barrier corresponding to D_{3h} symmetry.

Another electron diffraction study of $MoCl_5$ [216] concluded that the vapor is either a mixture of molecules with D_{3h} and C_{4v} symmetry (trigonal bipyramid and tetragonal pyramid, see Fig. 15), or it is such a mixture with

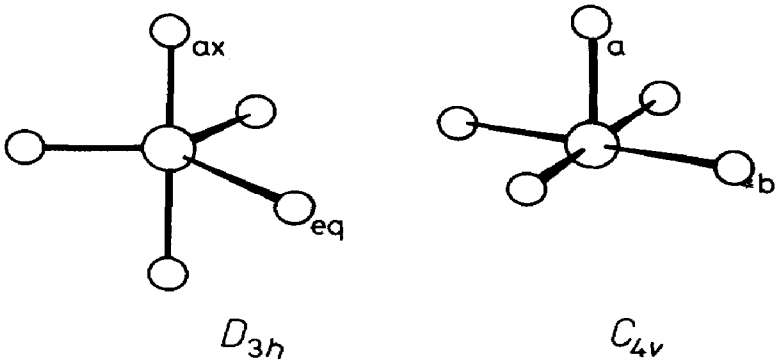

Fig. 15. Two possible models for an MX_5 pentahalide.

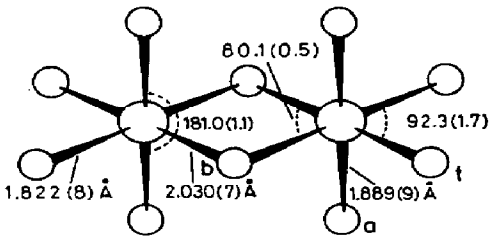

Fig. 16. Molecular configuration of dimeric $(MX_5)_2$ pentahalides, with the geometrical parameters of $(AuF_5)_2$.

some dimers present in addition. The first model could be accepted supposing large-amplitude motion. Employing a relatively rigid model, however, some dimer content had to be introduced. The dimer was supposed to consist of two C_{4v} symmetry units connected by a Mo–Mo bond, and D_{4d} symmetry was assumed for the molecule. This is so far the only example among metal halides of dimer formation with a metal–metal bond instead of halogen bridges. The first model with large amplitudes of vibration, however, can be perhaps considered a result of averaging different distorted configurations, again as a consequence of the Jahn–Teller effect. This model seems very plausible indeed.

(ii) Dimers

Dimeric species were found in the vapors of AuF_5 by mass spectrometric [217] and electron diffraction [218] studies, and in the vapors of UCl_5 by spectroscopy [219]. The suggested geometry is shown in Fig. 16 with the geometrical parameters of $(AuF_5)_2$. The metal atoms have a distorted octahedral bond configuration.

(iii) Trimers

Several pentahalides appear to have trimeric molecules in their vapor, and this is the most common form for vapor phase pentafluorides. SbF_5 consists mainly of trimeric species in the vapor [220]. The early electron diffraction studies of NbF_5 and TaF_5 vapors [221] at 300–320 K were interpreted with tetrameric species, which were related to the corresponding crystal structures [222]. Subsequent mass spectrometric studies of TaF_5 [223] indicated the presence primarily of trimers in the vapor. An electron diffraction reinvestigation of both compounds [220,224] provided conclusive evidence for trimeric species in the vapors under the experimental conditions.

Molybdenum pentafluoride was also found to be in a trimeric form in the vapor at lower temperatures by mass spectrometry [225]. The electron

TABLE 17

Geometrical parameters of trimeric pentahalides

	$(SbF_5)_3$ [220]	$(NbF_5)_3$ [220]	$(TaF_5)_3$ [224]	$(MoF_5)_3$ [a] [226]	$(AuF_5)_3$ [218]
r_α (M–F)$_t$ (Å) [b]	1.811(2)	1.810(2)	1.823(5)	1.804(35)	1.822(8)
r_α(M–F)$_a$ (Å)	1.811(2)	1.810(2)	1.846(5)	1.821(30)	1.889(9)
r_α(M–F)$_b$ (Å)	2.044(4)	2.046(4)	2.062(2)	2.012(10)	2.030(7)
$\angle_\alpha F_a$–M–F_a (deg)	161.6(17)	162.5(14)	173.1(21)	160.1(10)	193.1(32)
$\angle_\alpha F_t$–M–F_t (deg)	98.2(19)	102.9(12)	96.4(15)	100.5(21)	75.3(65)
$\angle_\alpha F_b$–M–F_b (deg)	81.5(15)	82.0(10)	83.5(6)	79.4(11)	115.7(11)
r_α(M ··· M) (Å) [c]	3.946	4.017	4.038	3.966	3.590

[a] r_a. [b] For definition of the different bond distances see Fig. 17. [c] Calculated from the other parameters.

diffraction data [226], however, could only be interpreted by these species if the presence of the hydrolysis product, $MoOF_4$, was also allowed for in the analysis. The vapors of AuF_5 contain trimeric species as well as dimers according to the electron diffraction study [218].

The trimers have a six-membered ring structure with alternating metal and fluorine atoms in the ring and three different types, axial, terminal and bridging metal–halogen bonds as shown in Fig. 17. The geometrical parameters are given in Table 17. The rings were found to be planar in $(NbF_5)_3$, $(TaF_5)_3$, $(MoF_5)_3$ and $(AuF_5)_3$, and considerably puckered in $(SbF_5)_3$. A C_{3v} and a C_s symmetry model gave about equally good agreement with the experiment for the antimony derivative. The important geometrical parameters, however, were practically invariant to the choice of the model. It has been suggested [227] that *d*-orbital participation in the bonding of transition metal pentafluorides may provide a π-type delocalized molecular orbital over the ring favoring planar conformation. However, such molecular orbitals would not be favorable in $(SbF_5)_3$ with the full $4d$ orbitals of the Sb atom.

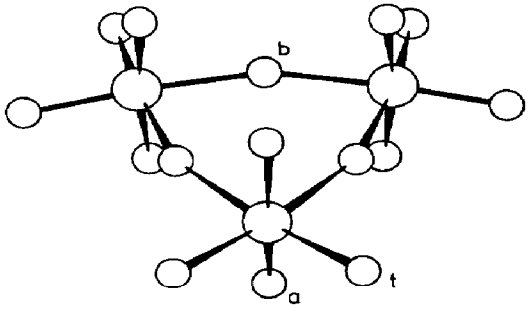

Fig. 17. Molecular configuration of trimeric $(MX_5)_3$ pentahalides.

Comparing the geometry of $(AuF_5)_3$ with those of $(SbF_5)_3$, $(NbF_5)_3$, $(TaF_5)_3$ and $(MoF_5)_3$, the most important difference is the very short metal · · · metal distance in $(AuF_5)_3$. The relatively large F_b–Au–F_b angle in the ring, 115.7(11)°, compared with the same angles of around 80° in the other trimers, is consistent with this short Au · · · Au separation.

Since the pentahalides usually form molecular crystals, it is interesting to compare the condensed phase and vapor phase geometries. The degree of association increases in the liquid and crystal structures. Thus, for example, whereas molybdenum, niobium, tantalum or tungsten pentachlorides are monomeric in the vapor, their liquid spectra indicate the presence of predominantly dimeric species [70]. The vapors of SbF_5, NbF_5 and TaF_5 contain trimers, whereas the crystals are built of tetrameric units.

G. HEXAHALIDES AND HEPTAHALIDES

The hexahalides are supposed to have a regular octahedral configuration and their vibrational spectra are interpreted accordingly [23]. The electron diffraction studies carried out so far have not detected any deviation from this high symmetry. Some of the hexahalides, such as ReF_6 and OsF_6, have a degenerate electronic ground state which could allow Jahn–Teller distortions, although such distortions have not been detected. As was discussed before, the dynamic nature of these distortions may keep them concealed. The bond distances are collected in Table 18 for all MX_6 molecules studied to date. Their variations correspond to expectation.

One heptahalide, ReF_7, will also be mentioned here. The most symmetrical model for this molecule would be a pentagonal bipyramid with D_{5h} symmetry. Vibrational spectra [232] were interpreted with this symmetry.

TABLE 18

Bond lengths in metal hexahalides

MX_6	r(M–X) (Å)	Reference
MoF_6	1.820(3) [a]	228
WF_6	1.832(3) [a]	228
	1.833(8) [b]	229
ReF_6	1.832(4) [a]	230
OsF_6	1.831(8) [b]	229
IrF_6	1.830(8) [b]	229
UF_6	1.999(3) [a]	231
	1.996(8) [b]	229
NpF_6	1.981(8) [b]	229
PuF_6	1.971(10) [b]	229

[a] r_g. [b] r_a.

Molecular beam deflection [233], however, was not compatible with such a high symmetry.

The apparent molecular symmetry from electron diffraction [234] is lower, C_2 or C_s, owing to "pseudorotation". Vibrational displacements carry the molecule from C_2 to C_s and again to C_2 symmetry. This motion closely resembles the pseudorotation of cyclopentane. The mean Re–F bond length is 1.835(5) Å.

H. COMPLEX METAL HALIDES

Aluminum chloride and other Lewis acid halides form volatile metal halide complexes with almost all metal halides. These vapor complexes have been extensively studied by different techniques owing to their practical importance in halogen metallurgy [7,70,235–238]. Most of these metal halide complexes have a very low concentration in the vapor. They can be identified by spectroscopic and mass spectrometric studies, and often their symmetry and general configuration can be determined or predicted. These studies have been extensively reviewed elsewhere [239].

These less abundant vapor complexes, however, cannot be studied by electron diffraction because of their small contribution to the electron scattering. Only some trifluoroberyllates, $AlkBeF_3$, Alk = Li [240], Na [241], K [241], and several tetrahaloaluminates (see later) and related compounds ($KYCl_4$ [242], $TlInCl_4$ [243]) have been investigated. The results published

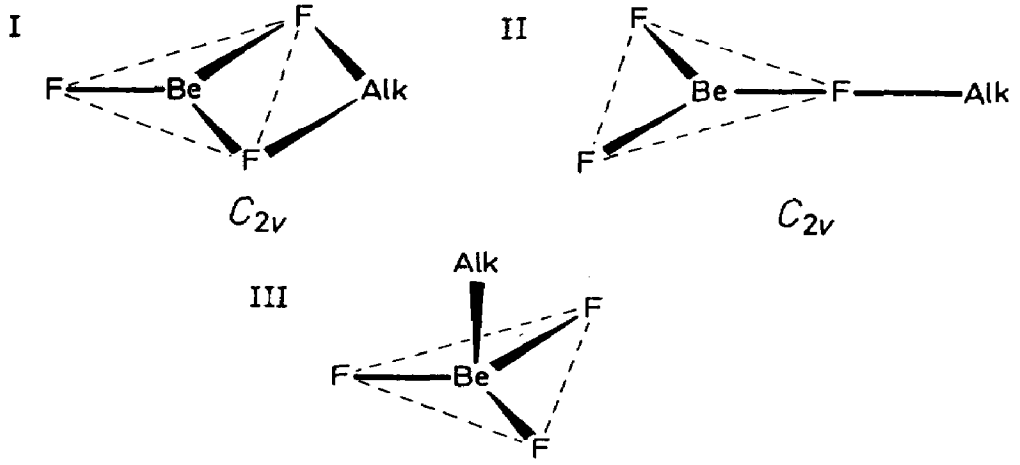

Fig. 18. Molecular models for alkali trifluoroberyllates.

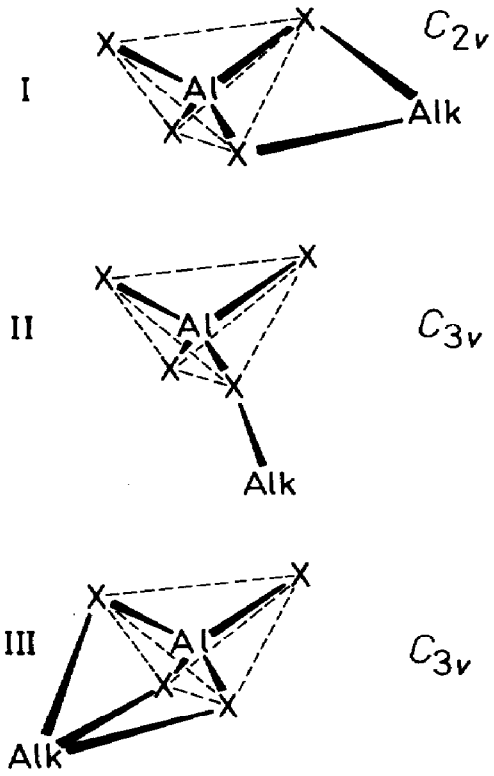

Fig. 19. Possible models of alkali tetrahaloaluminates. Model I is preferred according to both experimental and theoretical evidence.

TABLE 19

Geometrical parameters of alkali tetrafluoroaluminates, $AlkAlF_4$

	Li [a] [244]	Na [b] [245]	K [c] [246]	Rb [c] [247]	Cs [c] [247]
$r(Al–F)_t$ (Å)	1.673	1.69(2)	1.695(8)	1.696(5)	1.695(6)
$r(Al–F)_b$ (Å)	1.764		1.695(10)		
r(Alk–F) (Å)	1.790	2.11(2)	2.525(14)	2.64(3)	2.84(9)
r_e(Alk–F) (Å) [d]	1.573	1.926	2.172	2.270	2.346
	1.564				
r_e(Alk–F) (Å) [e]	1.68	1.90	2.25	2.35	2.55
r(Alk · · · Al) (Å)	2.647	2.58(3)	3.137(14)	3.32(7)	3.51(8)
$\angle F_b–Al–F_b$ (deg)	84.5	[f]	103.1(11)	[f]	[f]
$\angle F_t–Al–F_t$ (deg)	118.8	[f]	117.9(8)	[f]	[f]
$\angle F_b–Alk–F_b$ (deg)	83.0	81.7(20)	63.4(3)	62.8(13)	57.5(35)

[a] r_e, ab initio calculation. [b] r_a. [c] r_g. [d] Distance in the gaseous alkali halide: LiF upper value, ab initio [244]; lower value, microwave spectroscopy [23]; all others, microwave spectroscopy [23]. [e] Distance in the Alk_2X_2 dimer, from calculation [30]. [f] AlF_4 unit supposed to be tetrahedral.

TABLE 20

Bond distances in $AlkAlCl_4$ molecules

	K [a] [248]	Rb [249]	Cs [249]
r_g(Al–Cl) (Å)	2.153(6)	2.151(6)	2.149(9)
r_g(Alk–Cl) (Å)	2.98(5)	3.16(3)	3.31(7)
r_e(Alk–Cl) (Å) [b]	2.667	2.787	2.906
r_e(Alk–Cl) (Å) [c]	2.84	2.99	3.17
r_g(Alk · · · Al) (Å)	3.71(7)	3.80(5)	3.85(10)

[a] For an earlier study of this molecule see ref. 250. [b] Distance in the gaseous alkali halide, microwave spectroscopy [23]. [c] Distance in the Alk_2X_2 dimer, from calculation [30].

before 1974 have been reviewed [21]. From among the models tested for $AlkBeF_3$ and shown in Fig. 18, model **I** gave the best agreement with experiment.

Possible models for the $AlkAlX_4$ complexes are shown in Fig. 19. All three agree in having an X_4 tetrahedron around the aluminum atom; only the linkages to the alkali atom are different. Fluoride and chloride complexes have been studied recently and their geometrical parameters are given in Tables 19 and 20.

The configuration of the $AlkAlX_4$ molecules studied so far is a bidentate structure with C_{2v} symmetry (model **I** in Fig. 19). A C_s configuration was found as the best static model for $KAlF_4$ and $NaAlF_4$, with the F_b–Alk–F_b triangle twisted with respect to the F_b–Al–F_b plane by 26° (**6**). This twist is

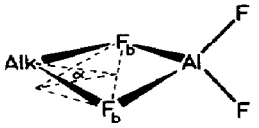

(**6**)

supposed again to be a consequence of large-amplitude vibrations of the four-membered ring and is not at variance with a C_{2v} symmetry equilibrium structure for these molecules.

The bonds between the alkali metal and the bridging halogen are considerably longer, by 0.2–0.5 Å, than the bonds in the corresponding free alkali halides. They are also longer than the Alk–X bonds of the Alk_2X_2 dimers. The Alk–X_b distances have unusually large amplitudes of vibration for a chemical bond, 0.15–0.25 Å. All this is in agreement with the spectroscopic results on the alkali tetrafluoroaluminates [238], indicating very small stretching force constants for these bonds, viz. 0.66, 0.36, 0.25, 0.18 and 0.15

mdyn $Å^{-1}$ for the lithium, sodium, potassium, rubidium and cesium derivatives respectively. These features point to a rather weak linkage between the alkali and halogen atoms. This "weakness", however, does not necessarily mean thermodynamic instability [2 (g)].

The structural conclusions for these molecules have been rationalized by a dynamic model involving polytopic bonds [2 (g),251]. The alkali atom has great mobility and belongs to all four halogen atoms in this description, whereas the AlX_4 unit is rather rigid and has T_d symmetry. The unperturbed T_d symmetry of the AlX_4 fragment, however, is not supported by other experimental and theoretical evidence. There are indications for a distorted AlX_4 fragment in these molecules. Unfortunately the terminal and bridging bonds could not be distinguished in the electron diffraction analyses. The mean lengths are about the same in all groups and are longer than the corresponding bond lengths in the monomers (see Table 10). The mean Al–Cl distances in tetrachloroaluminates are the same as the mean of the terminal and bridging bond lengths of the Al_2Cl_6 dimer (Table 11). The force constants are quite different [238], also indicating a relatively weaker bridging bond, similar to that in the Al_2X_6-type dimers. Ab initio calculations on $LiAlF_4$ also predicted a longer Al–F bridging bond [244]. The bond angles in $KAlF_4$ from electron diffraction and in $LiAlF_4$ from calculation also indicate a distortion similar to that described above.

The interaction between the alkali cation and the tetrahaloaluminate anion was found to be very weak in melts [252]. The anions have a regular tetrahedral shape. This regular tetrahedral arrangement undergoes C_{2v} distortion in the vapor phase according to Huglen et al. [238]. This is indicated by the splitting of the ν_3 and the occurrence of the ν_1 stretching frequencies in the IR spectra. Moreover, this distortion depends on the cation. More-polarizing cations cause larger distortions, expressed by an increased splitting of the ν_3 stretching frequencies on passing from cesium to lithium [238].

A splitting of frequencies owing to the large polarizing power of the small cations can also be observed, although to a lesser extent, for alkalihaloaluminate melts [252]. The simple model [251] of polytopic bonds in these structures, however, does not make use of cation polarizability.

Structure analysis combining different techniques will facilitate a better understanding of these interesting geometries. They are expected to become the subjects of intensive research in the future.

Aluminum halide complexes, with other than alkali metals, have been extensively studied by different spectroscopic techniques [70] as well as by ab initio calculations [253]. The most common composition of these complexes is $MX_2 \cdot Al_2Cl_6$.

I. CONCLUDING REMARKS

The amount of experimental and computational information on the molecular geometry of gas-phase metal halides is steadily growing as may be seen in the present review. We have also tried to show, however, the ambiguities and puzzles that also seem to characterize this area of structural chemistry. Further progress is expected from the combined application of various techniques in gaining more extensive and reliable data on gaseous metal halides. At this time the general types of metal halide molecules may be summarized in a few structures depicted through some representative molecules:

Monohalides (LiF, CuCl)

Monomer Dimer Trimer

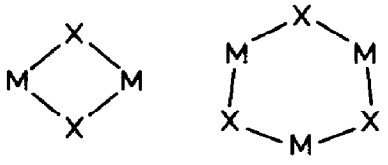

Dihalides

Linear MX_2 ($FeCl_2$, $CaBr_2$)

Monomer Dimer

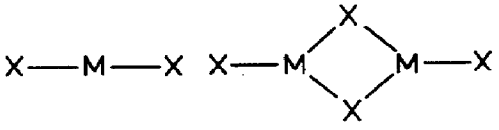

Bent MX_2 (GeF_2, SnF_2)

Monomer Dimer

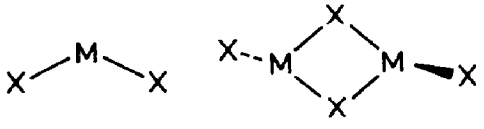

Trihalides

Planar MX_3 ($AlCl_3$, $GaCl_3$)

Monomer Dimer

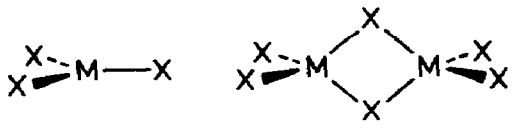

Pyramidal MX_3 ($SbCl_3$, $LaBr_3$)

Monomer

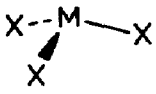

Tetrahalides

Tetrahedral MX_4 ($GeCl_4$, TiF_4)

Monomer

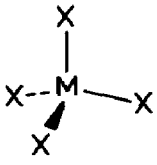

Non-tetrahedral MX_4

Monomer

TeF_4 $ThCl_4$

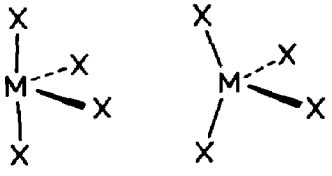

Pentahalides

Monomer	Dimer	Trimer
$SbCl_5$	$(AuF_5)_2$	$(SbF_5)_3$
$NbCl_5$	$(UCl_5)_2$	$(NbF_5)_3$

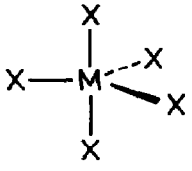

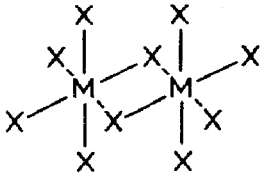

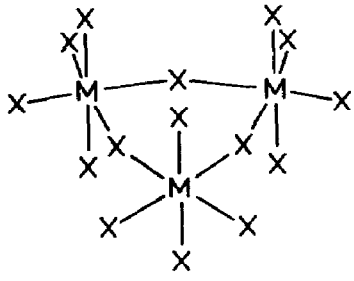

Hexahalides

Monomer MX_6 (WF_6, ReF_6)

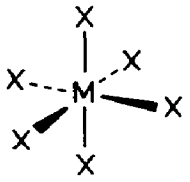

REFERENCES

1 A. Büchler, J.L. Stauffer and W. Klemperer, J. Am. Chem. Soc., 86 (1964) 4544.

2 J.W. Hastie (Ed.), Symposium on Characterization of High Temperature Vapors and Gases, National Bureau of Standards, Special Publication 561, 1979. Several of the papers (refs. 2 (a)–2 (g)) in this reference discuss this question.
(a) R.H. Hauge and J.L. Margrave, Matrix Isolation Studies of High Temperature Species, p. 495 in ref. 2.
(b) I.R. Beattie and D.A. Greenhalgh, The Determination of the Molecular Shapes of High Temperature Species, p. 597 in ref. 2.
(c) M.C. Drake and G.M. Rosenblatt, Raman Spectroscopy in High Temperature Chemistry, p. 609 in ref. 2.
(d) T. Torring and E. Tiemann, Rotational Spectroscopy of High Temperature Molecules, p. 695 in ref. 2.
(e) W. Weltner, Jr., Transition-metal Molecules and Walsh's Rules Rationalization of Optical and ESR Data, p. 587 in ref. 2.
(f) G.N. Papatheodorou, Resonance Raman Spectra of Metal Halide Vapor Complexes, p. 647 in ref. 2.
(g) V.P. Spiridonov and E.Z. Zasorin, Modern High-temperature Electron Diffraction, p. 711 in ref. 2.

3 J. Tremmel and I. Hargittai, Gas electron diffraction experiment, in I. Hargittai and M. Hargittai (Eds.), Stereochemical Applications of Gas-phase Electron Diffraction, Part A, VCH, New York, 1988, p. 191.

4 J.L. Margrave (Ed.), The Characterization of High Temperature Vapors, Wiley, New York, 1967.

5 J.W. Hastie, High Temperature Vapors: Science and Technology, Academic Press, New York, 1975.

6 D.L. Hildenbrand and D.D. Cubicciotti (Eds.), Proc. Symp. on High Temperature Metal Halide Chemistry, Electrochemical Society, Princeton, NJ, 1978.

7 H. Schäfer, Angew. Chem., 88 (1976) 775.

8 L. Brewer, Behavior of halides at high temperatures, in D.L. Hildenbrand and D.D. Cubicciotti (Eds.), Proc. Symp. on High Temperature Metal Halide Chemistry, Electrochemical Society, Princeton, NJ, 1978, p. 177.

9 J.S. Ogden and R.S. Wyatt, J. Chem. Soc., Dalton Trans., (1987) 859.

10 M. Jacox and D.E. Milligan, J. Chem. Phys., 51 (1969) 4143.

11 I. Eliezer and A. Reger, Coord. Chem. Rev., 9 (1972/73) 189.

12 M.L. Lesiecki and J.S. Shirk, J. Chem. Phys., 56 (1972) 4171.
13 J.S. Shirk and A.E. Shirk, J. Chem. Phys., 64 (1976) 910.
14 R.H. Hauge, J.L. Margrave and A.S. Kanaan, J. Chem. Soc., Faraday Trans., 71 (1975) 1082.
15 M. Hargittai, Metal halides, in I. Hargittai and M. Hargittai (Eds.), Stereochemical Applications of Gas-phase Electron Diffraction, Part B, VCH, New York, 1988, p. 383.
16 K. Kuchitsu, in I. Hargittai and W.J. Orville-Thomas (Eds.), Diffraction Studies on Non-crystalline Substances, Elsevier, Amsterdam, 1981.
17 V.P. Spiridonov, Kem. Kozl., 37 (1972) 399 and references therein.
18 H.F. Schaefer, J. Mol. Struct., 76 (1981) 117.
19 I. Hargittai, S. Bohatka, J. Tremmel and I. Berecz, Hung. Sci. Instrum., 50 (1980) 51.
20 V.P. Spiridonov, in I. Hargittai and W.J. Orville-Thomas (Eds.), Diffraction Studies on Non-crystalline Substances, Elsevier, Amsterdam, 1981.
21 M. Hargittai and I. Hargittai, The Molecular Geometries of Coordination Compounds in the Vapor Phase, Akademiai Kiado, Budapest, and Elsevier, Amsterdam, 1977.
22 P. Davidovits and D.L. McFadden (Eds.), Alkali Halide Vapors, Academic Press, New York, 1979.
23 K.S. Krasnov (Ed.), Molecular Constants of Inorganic Compounds, Khimiya, Leningrad, 1979 (in Russian).
24 V.G. Solomonik, K.S. Krasnov, G.V. Girichev and E.Z. Zasorin, Zh. Strukt. Khim., 20 (1979) 427.
25 R.J. Mawhorter, M. Fink and J.G. Hartley, J. Chem. Phys., 83 (1985) 4418.
26 J.G. Hartley and M. Fink, J. Chem. Phys., submitted for publication.
27 A.F. Wells, Structural Inorganic Chemistry, 4th edn., Clarendon Press, Oxford, 1975.
28 L.R. Maxwell, S.B. Hendricks and V.M. Mosley, Phys. Rev., 52 (1937) 968.
29 T.P. Martin and H. Schaber, J. Chem. Phys., 68 (1978) 4299; H. Schaber and T.P. Martin, J. Chem. Phys., 70 (1979) 2029.
30 D.O. Welch, O.W. Lazareth and G.J. Dienes, J. Chem. Phys., 64 (1976) 835.
31 P.N. Swepston, H.L. Sellers and L. Schäfer, J. Chem. Phys., 74 (1981) 2372.
32 V.G. Solomonik, V.M. Ozerova and A.I. Boldyrev, Zh. Neorg. Khim., 27 (1982) 1891.
33 T.P. Martin, J. Chem. Phys., 69 (1978) 2036.
34 T.P. Martin, Phys. Rep., 95 (1983) 167.
35 N.N. Greenwood and A. Earnshaw, Chemistry of the Elements, Pergamon, Oxford, 1984.
36 P.L. Radloff and G.N. Papatheodorou, J. Chem. Phys., 72 (1980) 992; P.L. Radloff and G.N. Papatheodorou, Raman spectra of indium halide vapors, in D.L. Hildenbrand and D.D. Cubicciotti (Eds.), Proc. Symp. on High Temperature Metal Halide Chemistry, Electrochemical Society, Princeton, NJ, 1978, p. 320.
37 N.I. Giricheva, V.M. Petrov, G.V. Girichev, V.A. Titov and T.P. Chusova, in G.V. Kulikova (Ed.), Study of the Structure and Energetics of Molecules, Ivanovo, 1986, p. 81 (in Russian).
38 D. Cubicciotti, High Temp. Sci., 2 (1970) 65.
39 F.J. Keneshea and D. Cubicciotti, J. Phys. Chem., 69 (1965) 3910; 71 (1967) 1958.
40 J.M. Brom and H.F. Fransen, J. Chem. Phys., 54 (1971) 2874 and references therein.
41 J.L. Dehmer, J. Berkowitz and L.C. Cusachs, J. Chem. Phys., 58 (1973) 5681.
42 M.G. Fickes, R.C. Slater, W.G. Becker and R.C. Stern, Chem. Phys. Lett., 24 (1974) 105.
43 J.S. Muenter, Chem. Phys. Lett., 26 (1974) 97.
44 V.G. Solomonik, E.Z. Zasorin, G.V. Girichev and K.S. Krasnov, Izv. Vyssh. Uchebn. Zaved., Khim. Khim. Tekhnol., 17 (1974) 136.
45 M.L. Lesiecki and J.W. Nibler, J. Chem. Phys., 63 (1975) 3452.

46 M. Guido, G. Balducci, G. Gigli and M. Spoliti, J. Chem. Phys., 55 (1971) 4566.
47 v.G. Krabbes and H. Oppermann, Z. Anorg. Allg. Chem., 435 (1977) 33.
48 T.E. Joyce and E.J. Rolinski, J. Phys. Chem., 76 (1972) 2310.
49 T.P. Martin and H. Schaber, J. Chem. Phys., 73 (1980) 3541.
50 C.-H. Wong and V. Schomaker, J. Phys. Chem., 61 (1957) 358.
51 E. Vajda, M. Hargittai, J. Tremmel and I. Hargittai, unpublished results.
52 B.S. Butaev, A.G. Gershikov and V.P. Spiridonov, Vestn. Mosk. Univ. Ser. Khim., 19 (1978) 734.
53 J. Berkowitz and J.R. Marquart, J. Chem. Phys., 37 (1962) 1853.
54 v.H.H. Emmons, D. Kiessling and W. Horlbeck, Z. anorg. allg. Chem., 488 (1982) 219.
55 V.V. Kasparov, Yu.S. Ezhov and N.G. Rambidi, Zh. Strukt. Khim., 21 (1980) 41.
56 V.V. Kasparov, Yu.S. Ezhov and N.G. Rambidi, Zh. Strukt. Khim., 20 (1979) 260.
57 M.L. Lesiecki and J.W. Nibler, J. Chem. Phys., 64 (1976) 871.
58 M. Guido and G. Gigli, J. Chem. Phys., 65 (1976) 1397.
59 V.P. Spiridonov, A.B. Altman, A.G. Gershikov and G.V. Romanov, Abstracts of Papers, 2nd Conf. on the Determination of Molecular Structure by Microwave Spectroscopy and Electron Diffraction, Tubingen, 1980.
60 V.P. Spiridonov, A.G. Gershikov, A.B. Altman, G.V. Romanov and A.A. Ivanov, Chem. Phys. Lett., 77 (1981) 41.
61 V.I. Baikov, Opt. Spektrosk., 25 (1968) 356.
62 Y. Hase and Y. Takahata, An. Acad. Bras. Cienc., 54 (1982) 502; 55 (1983) 23.
63 L. Wharton, R.A. Berg and W. Klemperer, J. Chem. Phys., 39 (1963) 2023.
64 V. Calder, D.E. Mann, K.S. Seshadri, M. Allavena and D. White, J. Chem. Phys., 51 (1969) 2093.
65 E. Vajda, M. Hargittai, I. Hargittai, J. Tremmel and J. Brunvoll, Inorg. Chem., 26 (1987) 1171.
66 V.V. Kasparov, Yu.S. Ezhov and N.G. Rambidi, Zh. Strukt. Khim., 20 (1979) 341.
67 D. White, G.V. Calder, S. Hemple and D.E. Mann, J. Chem. Phys., 59 (1973) 6645.
68 P.A. Akishin, V.P. Spiridonov and G.A. Sobolev, Dokl. Akad. Nauk SSSR, 118 (1958) 1134; P.A. Akishin and V.P. Spiridonov, Kristallografiya, 2 (1957) 475; P.A. Akishin, V.P. Spiridonov and G.A. Sobolev, Zh. Fiz. Khim., 31 (1957) 648 and references therein.
69 M. Spoliti, G. De Maria, L. D'Alessio and M. Maltese, J. Mol. Struct., 67 (1980) 159.
70 M.H. Brooker and G.N. Papatheodorou, Vibrational spectroscopy of molten salts and related glasses and vapors in G. Mamantov (Ed.), Advances in Molten Salt Chemistry, Vol. 5, Elsevier, Amsterdam, 1983.
71 B. Saha, K. Hilpert and L. Bencivenni, in J.F.J. Todd (Ed.) Advances in Mass Spectrometry, Vol. 10B, Wiley, New York, 1986.
72 M.C. Drake and G.M. Rosenblatt, J. Electrochem. Soc., 126 (1979) 1387.
73 R.J. Gillespie, Molecular Geometry, Van Nostrand Reinhold, London, 1972.
74 A.D. Walsh, J. Chem. Soc., (1953) 2266.
75 E.F. Hayes, J. Phys. Chem., 70 (1966) 3740.
76 J.L. Gole, A.K.Q. Siu and E.F. Hayes, J. Chem. Phys., 58 (1973) 857.
77 M. Hargittai, J. Tremmel and I. Hargittai, Inorg. Chem., 25 (1986) 3163.
78 K. Hilpert, L. Bencivenni and B. Saha, J. Chem. Phys., 83 (1985) 5227.
79 N.Yu. Subbotina, G.V. Girichev, A.G. Gershikov and E.G. Rakov, 8th All-Union Symp. on Inorganic Fluoride Chemistry, Abstract, Nauka, Moscow, 1987, p. 357.
80 V.M. Petrov, A.N. Utkin, G.V. Girichev and A.A. Ivanov, Zh. Strukt. Khim., 26 (1985) 52.
81 K. Kashiwabara, S. Konaka and M. Kimura, Bull. Chem. Soc. Jpn., 46 (1973) 410.

82 V.P. Spiridonov, A.G. Gershikov and B.S. Butaev, J. Mol. Struct., 52 (1979) 53; A.G. Gershikov, Zh. Strukt. Khim., 25 (1984) 30.
83 A. Loewenschuss and A. Givan, Ber. Bunsenges. Phys. Chem., 82 (1978) 69.
84 A. Loewenschuss, A. Ron and O. Schnepp, J. Chem. Phys., 49 (1968) 272; 50 (1969) 2502.
85 A. Givan and A. Loewenschuss, J. Chem. Phys., 65 (1976) 1851.
86 A. Givan and A. Loewenschuss, J. Mol. Struct., 48 (1978) 325.
87 A. Büchler, J.L. Stauffer and W. Klemperer, J. Chem. Phys., 40 (1964) 3471.
88 D.R. Yarkony and H.F. Schaefer, Chem. Phys. Lett., 15 (1972) 514.
89 H. Blasch, C. Hollister and J.W. Moskowitz, Chem. Phys. Lett., 4 (1969) 79.
90 M. Hargittai and A.R. Rossi, Inorg. Chem., 24 (1985) 4758.
91 D.W. Smith, Inorg. Chim. Acta, 22 (1977) 107.
92 J.W. Hastie, R.H. Hauge and J.L. Margrave, Ann. Rev. Phys. Chem., 21 (1970) 475; J. Chem. Soc., Chem. Commun., (1969) 1452; High Temp. Sci., 1 (1969) 76; 3 (1971) 257.
93 T.C. De Vore, R.J. Van Zee and W. Weltner, Jr., An investigation of the first row transition-metal fluoride molecules using ESR spectroscopy, in D.L. Hildenbrand and D.D. Cubicciotti (Eds.), Proc. Symp. on High Temperature Metal Halide Chemistry, Electrochemical Society, Princeton, NJ, 1978, p. 187.
94 V.M. Kovba, Zh. Neorg. Khim., 28 (1983) 2689.
95 D.W. Green, D.P. McDermott and A. Bergman, J. Mol. Spectrosc., 98 (1983) 11.
96 J. Tremmel and M. Hargittai, unpublished results.
97 E.Z. Zasorin, A.G. Gershikov, V.P. Spiridonov and A.A. Ivanov, Zh. Strukt. Khim., 28 (1987) 56.
98 A.G. Gershikov, N.Yu. Subbotina and G.V. Girichev, Zh. Strukt. Khim., 27 (1986) 36.
99 (a) I. Hargittai, J. Tremmel and Gy. Schultz, J. Mol. Struct., 26 (1975) 116.
(b) J. Tremmel, A.A. Ivanov, Gy. Schultz, I. Hargittai, S.J. Cyvin and A. Eriksson, Chem. Phys. Lett., 23 (1973) 533.
100 M. Hargittai, M. Kolonits, J. Tremmel and I. Hargittai, to be published.
101 M. Hargittai and I. Hargittai, J. Mol. Spectrosc., 108 (1984) 155.
102 E. Vajda, J. Tremmel and I. Hargittai, J. Mol. Struct., 44 (1978) 101.
103 L. Eddy, Dissertation, Oregon State University, Corvallis, OR, 1973.
104 M. Hargittai, I. Hargittai and J. Tremmel, Chem. Phys. Lett., 83 (1981) 207.
105 M. Hargittai, O.V. Dorofeeva and J. Tremmel, Inorg. Chem., 24 (1985) 245.
106 Zs. Molnar, Gy. Schultz, J. Tremmel and I. Hargittai, Acta Chim. Acad. Sci. Hung., 86 (1975) 223.
107 (a) I.A. Ratkovskii, T.A. Pribitkova and N.V. Galickii, Teplofiz. Vys. Temp., 12 (1974) 731.
(b) I.A. Ratkovskii, L.N. Novikova, L.Y. Krisko and E.M. Rokashevich, Zh. Fiz. Khim., 50 (1976) 520.
108 (a) M. Hargittai, O.V. Dorofeeva and J. Tremmel, Inorg. Chem., 24 (1985) 3963.
(b) M. Hargittai, O.V. Dorofeeva and J. Tremmel, to be published.
109 R.C. Schoonmaker, A.H. Friedman and R.F. Porter, J. Chem. Phys., 31 (1959) 1586.
110 C.W. Dekock, R.D. Wesley and D.D. Ratke, High Temp. Sci., 4 (1972) 41.
111 J.W. Hastie, R.H. Hauge and J.L. Margrave, High Temp. Sci., 3 (1971) 56.
112 I.R. Beattie, J.S. Ogden and R.S. Wyatt, J. Chem. Soc., Dalton Trans., (1983) 2343.
113 E.V. Erokhin, V.P. Spiridonov, A.G. Gershikov, N.I. Raevskii and Yu.M. Kiselev, Zh. Strukt. Khim., 25 (1984) 75.
114 W.H. Kirchhoff, D.R. Lide and F.X. Powell, J. Mol. Spectrosc., 47 (1973) 491.
115 H. Shoji, T. Tanaka and E. Hirota, J. Mol. Spectrosc., 47 (1973) 268.

116 H. Takeo, R.F. Curl and P.W. Wilson, J. Mol. Spectrosc., 38 (1971) 464.
117 I. Hargittai, Gy. Schultz, J. Tremmel, N.D. Kagramanov, A.K. Maltsev and O.M. Nefedov, J. Am. Chem. Soc., 105 (1983) 2895.
118 Gy. Schultz, J. Tremmel, I. Hargittai, I. Berecz, S. Bohatka, N.D. Kagramanov, A.K. Maltsev and O.M. Nefedov, J. Mol. Struct., 55 (1979) 207.
119 Gy. Schultz, J. Tremmel, I. Hargittai, N.D. Kagramanov, A.K. Maltsev and O.M. Nefedov, J. Mol. Struct., 82 (1982) 107.
120 A.A. Ishchenko, L.S. Ivashkevich, E.Z. Zasorin, V.P. Spiridonov and A.A. Ivanov, 6th Austin Symp. on Gas-phase Molecular Structure, 1976, A15; A.Ya. Nasarenko, V.P. Spiridonov, B.S. Butayev and E.Z. Zasorin, J. Mol. Struct., 119 (1985) 263.
121 A.V. Demidov, A.G. Gershikov, E.Z. Zasorin, V.P. Spiridonov and A.A. Ivanov, Zh. Strukt. Khim., 24 (1983) 9.
122 I. Hargittai, J. Tremmel, E. Vajda, A.A. Ishchenko, A.A. Ivanov, L.S. Ivashkevich and V.P. Spiridonov, J. Mol. Struct., 42 (1977) 147.
123 C.W. Bauschlicher, H.F. Schaefer and P.S. Bagus, J. Am. Chem. Soc., 99 (1977) 7106.
124 B. Delley and G. Solt, J. Mol. Struct., 139 (1986) 159.
125 H. Huber, E.P. Künding, G.A. Ozin and A. Vander Voet, Can. J. Chem., 52 (1974) 95.
126 J. Trotter, M. Akhtar and N. Bartlett, J. Chem. Soc. A, (1966) 30.
127 I. Novak and A.W. Potts, J. Chem. Soc., Dalton Trans., (1983) 2211.
128 K. Zmbov, J.W. Hastie and J.L. Margrave, Trans. Faraday Soc., 64 (1968) 861.
129 R.C. McDonald, H. Ho-Kuen Hau and K. Eriks, Inorg. Chem., 15 (1976) 762.
130 G.A. Ozin and A. Vander Voet, J. Chem. Soc., Chem. Commun., (1970) 896.
131 L. Fernholt, A. Haaland, R. Seip, R. Kniep and L. Korte, Z. Naturforsch., Teil B, 38 (1983) 1072.
132 L. Fernholt, A. Haaland, H.V. Volden and R. Kniep, J. Mol. Struct., 128 (1985) 29.
133 G.E. Vrieland and D.R. Stull, J. Chem. Eng. Data, 12 (1967) 532.
134 R.F. Porter and E.E. Zeller, J. Chem. Phys., 33 (1960) 858.
135 N.A. Zhegulskaya, V.B. Soltz and L.N. Sidorov, Zh. Fiz. Khim., 46 (1972) 1889.
136 Q. Shen, Ph.D. Thesis, Oregon State University, Corvallis, OR, 1974.
137 R. Hillel, A. Ait-Hou, M.P. Berthet and J. Bouix, J. Raman Spectrosc., 18 (1987) 259.
138 T. Tomita, C.E. Sjøgren, P. Klaeboe, G.N. Papatheodorou and E. Rytter, J. Raman Spectrosc., 14 (1983) 415.
139 C.E. Sjogren, P. Klaeboe and E. Rytter, Spectrochim. Acta, Part A, 40 (1984) 457 and references therein.
140 A.N. Utkin, G.V. Girichev, N.I. Giricheva and S.V. Khaustov, Zh. Strukt. Khim., 27 (1986) 43.
141 L. Curtiss, Int. J. Quantum Chem., 14 (1978) 709.
142 E.Z. Zasorin and N.G. Rambidi, Zh. Strukt. Khim., 8 (1967) 391.
143 V.P. Spiridonov, A.G. Gershikov, E.Z. Zasorin, N.I. Popenko, A.A. Ivanov and L.I. Ermolayeva, High Temp. Sci., 14 (1981) 285.
144 Y. Morino, T. Ukayi and T. Ito, Bull. Chem. Soc. Jpn., 39 (1966) 71.
145 N.I. Giricheva, V.M. Petrov, V.A. Titov and T.P. Chusova, Zh. Strukt. Khim., 27 (1986) 48.
146 S. Konaka, Bull. Chem. Soc. Jpn., 43 (1970) 3107.
147 F.B. Clippard and L.S. Bartell, Inorg. Chem., 9 (1970) 805.
148 S. Samdal, D.M. Barnhart and K. Hedberg, J. Mol. Struct., 35 (1976) 67.
149 (a) S. Konaka and M. Kimura, Bull. Chem. Soc. Jpn., 46 (1973) 404.
(b) V.V. Ugarov, Yu.Sh. Kalaichev and K.P. Petrov, Zh. Strukt. Khim., 26 (1985) 170.

150 A. Haaland, J. Hougen, S. Samdal and J. Tremmel, Acta Chem. Scand., Ser. A, in press.
151 S. Konaka and M. Kimura, Bull. Chem. Soc. Jpn., 46 (1973) 413.
152 A. Almenningen and T. Bjorvatten, Acta Chem. Scand., 17 (1963) 2573.
153 H.B. Bürgi, D. Stedman and L.S. Bartell, J. Mol. Struct., 10 (1971) 31.
154 K. Hedberg and M. Iwasaki, J. Chem. Phys., 36 (1962) 589.
155 E.W. Kaiser, W.E. Falconer and W. Klemperer, I. Chem. Phys., 56 (1972) 5392.
156 N.I. Giricheva, E.Z. Zasorin, G.V. Girichev, K.S. Krasnov and V.P. Spiridonov, Zh. Strukt. Khim., 17 (1976) 797.
157 R.H. Hauge, J.W. Hastie and J.L. Margrave, J. Less-Common Met., 23 (1971) 359.
158 J.W. Hastie, R.H. Hauge and J.L. Margrave, J. Chem. Phys., 51 (1969) 2648.
159 E.Z. Zasorin, A.A. Ivanov, V.P. Spiridonov and L.I. Ermolaeva, 8th All-Union Symp. on Inorganic Fluoride Chemistry, Abstract, Nauka, Moscow, 1987, p. 143.
160 M. Hargittai, M. Kolonits, J. Tremmel, J.-L. Fourquet and G. Ferey, Inorg. Chem., submitted for publication.
161 R.A. Frey, R.D. Werder and Hs.H. Günthard, J. Mol. Spectrosc., 35 (1970) 260.
162 A. Givan and A. Loewenschuss, J. Raman Spectrosc., 6 (1977) 84; A. Loewenschuss and A. Givan, Ber. Bunsenges. Phys. Chem., 82 (1978) 74.
163 Yu.S. Ezhov and S.A. Komarov, Zh. Strukt. Khim., 26 (1985) 178.
164 K. Rinke and H. Schäfer, Angew. Chem., 79 (1967) 650.
165 M. Hargittai, J. Tremmel and I. Hargittai, J. Chem. Soc., Dalton Trans., (1980) 87.
166 Yu.S. Ezhov and S.A. Komarov, Zh. Strukt. Khim., 26 (1985) 60.
167 V.V. Ugarov, V.S. Vinogradov, E.Z. Zasorin and N.G. Rambidi, Zh. Strukt. Khim., 12 (1971) 315.
168 L. Pauling, The Nature of the Chemical Bond, Cornell University Press, Ithaca, NY, 1960.
169 W.F. Howard and L. Andrews, Inorg. Chem., 14 (1975) 1726.
170 J.W. Hastie, R.H. Hauge and J.L. Margrave, J. Less-Common Met., 39 (1975) 309.
171 J.W. Wells, Jr., J.B. Gruber and M. Lewis, Chem. Phys. 24 (1977) 391.
172 R.D. Wesley and C.W. DeKock, J. Chem. Phys., 55 (1971) 3866.
173 O.P. Charkin and M.E. Dyatkina, Zh. Strukt. Khim., 5 (1964) 921.
174 K.S. Krasnov, G.V. Girichev, N.I. Giricheva, V.M. Petrov, T.G. Danilova, E.Z. Zasorin and N.I. Popenko, 7th Austin Symp. on Gas-phase Molecular Structure, Abstracts, 1978, p. 89.
175 G.V. Girichev, T.G. Danilova, N.I. Giricheva, K.S. Krasnov, V.M. Petrov, A.N. Utkin and E.Z. Zasorin, Izv. Vyssh. Uchebn. Zaved., Khim. Khim. Tekhnol., 21 (1978) 627.
176 T.G. Danilova, G.V. Girichev, N.I. Giricheva, K.S. Krasnov and E.Z. Zasorin, Izv. Vyssh. Uchebn. Zaved., Khim. Khim. Tekhnol., 20 (1977) 1069.
177 G.V. Girichev., T.G. Danilova, N.I. Giricheva, K.S. Krasnov and E.Z. Zasorin, Izv. Vyssh. Uchebn. Zaved., Khim. Khim. Tekhnol., 20 (1977) 1233.
178 N.I. Giricheva, E.Z. Zasorin, G.V. Girichev, K.S. Krasnov and V.P. Spiridonov, Izv. Vyssh. Uchebn. Zaved., Khim. Khim. Tekhnol., 20 (1977) 284.
179 N.I. Giricheva, E.Z. Zasorin, G.V. Girichev, K.S. Krasnov and V.P. Spiridonov, Izv. Vyssh. Uchebn. Zaved., Khim. Khim. Tekhnol., 17 (1974) 762.
180 N.I. Popenko, E.Z. Zasorin, V.P. Spiridonov and A.A. Ivanov, Inorg. Chim. Acta, 31 (1978) L371.
181 K.S. Krasnov, N.I. Giricheva and G.V. Girichev, Zh. Strukt. Khim., 17 (1976) 667.
182 Y. Morino, Y. Nakamura and T. Iijima, J. Chem. Phys., 32 (1960) 643.
183 G.G.B. Souza and J.D. Wieser, J. Mol. Struct., 25 (1975) 442.
184 H. Fujii and M. Kimura, Bull. Chem. Soc. Jpn., 43 (1970) 1933.

185 G.V. Girichev, V.M. Petrov, N.I. Giricheva and K.S. Krasnov, Zh. Strukt. Khim., 23 (1982) 56.
186 Y. Morino and H. Uehara, J. Chem. Phys., 45 (1966) 4543.
187 G.V. Girichev, E.Z. Zasorin, N.I. Giricheva, K.S. Krasnov and V.P. Spiridonov, Zh. Strukt. Khim., 18 (1977) 42.
188 V.M. Petrov, G.V. Girichev, N.I. Giricheva, O.K. Shaposhnikova and E.Z. Zasorin, Zh. Strukt. Khim., 20 (1979) 136.
189 A.N. Utkin, V.N. Petrova, G.V. Girichev and V.M. Petrov, Zh. Strukt. Khim., 27 (1986) 177.
190 G.V. Girichev, V.M. Petrov, N.I. Giricheva, A.N. Utkin and V.N. Petrova, Zh. Strukt. Khim., 22 (1981) 65.
191 L.S. Ivashkevich, A.A. Ishchenko, V.P. Spiridonov and G.V. Romanov, J. Mol. Struct., 51 (1979) 217.
192 H.A. Jahn and E. Teller, Proc. Roy. Soc. London, 161 (1937) 220.
193 I.B. Bersuker, Coord. Chem. Rev., 14 (1975) 357; I.B. Bersuker, The Jahn–Teller Effect and Vibronic Interactions in Modern Chemistry, Plenum, New York, 1984.
194 V.P. Spiridonov and G.V. Romanov, Vest. Mosk. Univ. Ser. Khim., 22 (1967) 118.
195 Yu.S. Ezhov and S.A. Komarov, Zh. Strukt. Khim., 25 (1984) 82.
196 C.J. Adams and A.J. Downs, Spectrochim. Acta, Part A, 28 (1972) 1841.
197 I.R. Beattie, J.R. Horder and R.J. Jones, J. Chem. Soc. A, (1970) 329.
198 I.C. Bowater, R.D. Brown and F.R. Burden, J. Mol. Spectrosc., 28 (1968) 451.
199 S.A. Arthers and I.R. Beattie, J. Chem. Soc., Dalton Trans., (1984) 819.
200 D.L. Hildenbrand, J. Chem. Phys., 66 (1977) 4788.
201 Yu.S. Ezhov, R.A. Akishin and N.G. Rambidi, Zh. Strukt. Khim., 10 (1969) 763.
202 G.V. Girichev, V.M. Petrov, N.I. Giricheva, E.Z. Zasorin, K.S. Krasnov and Yu.M. Kiselev, Zh. Strukt. Khim., 24 (1983) 70.
203 V.M. Petrov, G.V. Girichev, N.I. Giricheva, V.N. Petrova, K.S. Krasnov, E.Z. Zasorin and Yu.M. Kiselev, Dokl. Akad. Nauk SSSR, 259 (1981) 1399.
204 L.S. Ivashkevich, A.A. Ishchenko, V.P. Spiridonov, T.G. Strand, A.A. Ivanov and A.N. Nikolaev, Zh. Strukt. Khim., 23 (1982) 144.
205 K. Hagen, M.M. Gilbert, L. Hedberg and K. Hedberg, Inorg. Chem., 21 (1982) 2690.
206 A.A. Ishchenko, T.G. Strand, A.V. Demidov and V.P. Spiridonov, J. Mol. Struct., 43 (1978) 227.
207 A.V. Demidov, A.A. Ivanov, L.S. Ivashkevich, A.A. Ishchenko and V.P. Spiridonov, Chem. Phys. Lett., 64 (1979) 528.
208 B.W. McClelland, L. Hedberg and K. Hedberg, J. Mol. Struct., 99 (1983) 309.
209 K.W. Hansen and L.S. Bartell, Inorg. Chem., 4 (1965) 1775.
210 T.R. Dyke, A.A. Muenter, W. Klemperer and W.E. Falconer, J. Chem. Phys., 53 (1970) 3382.
211 R.S. Berry, J. Chem. Phys., 32 (1960) 933.
212 E.J. Jacob, L. Hedberg, K. Hedberg, H. Davis and G.L. Gard, J. Phys. Chem., 88 (1984) 1935.
213 E.G. Hope, P.J. Jones, W. Levason, J.S. Ogden, M. Tajik and J.W. Turff, J. Chem. Soc., Dalton Trans., (1985) 1443.
214 Yu.S. Ezhov and A.P. Sarvin, Zh. Strukt. Khim., 24 (1983) 57.
215 Yu.S. Ezhov and A.P. Sarvin, Zh. Strukt. Khim., 24 (1983) 149.
216 J. Brunvoll, A.A. Ishchenko, V.P. Spiridonov and T.G. Strand, Acta Chem. Scand., Ser. A, 38 (1984) 115.
217 M.J. Vasile, T.J. Richardson, F.A. Stevie and W.E. Falconer, J. Chem. Soc., Dalton Trans., (1976) 351.

218 J. Brunvoll, A.A. Ishchenko, A.A. Ivanov, G.V. Romanov, V.B. Sokolov, V.P. Spiridonov and T.G. Strand, Acta Chem. Scand., Ser. A, 36 (1982) 705.
219 G.N. Papatheodorou and D.A. Buttry, Inorg. Nucl. Chem. Lett., 15 (1979) 51.
220 J. Brunvoll, A.A. Ishchenko, I.N. Miakshin, G.V. Romanov, V.P. Spiridonov, T.G. Strand and V.F. Sukhoverkhov, Acta Chem. Scand., Ser. A, 34 (1980) 733.
221 G.V. Romanov and V.P. Spiridonov, Vest. Mosk. Univ. Ser. Khim., 23 (1968) 7.
222 A.J. Edwards, J. Chem. Soc., (1964) 3714.
223 A.V. Gusarov, L.N. Gorokhov and I.S. Gotkis, Adv. Mass Spectrom., 7 (1978) 666.
224 J. Brunvoll, A.A. Ishchenko, I.N. Miakshin, G.V. Romanov, V.B. Sokolov, V.P. Spiridonov and T.G. Strand, Acta Chem. Scand., Ser. A, 33 (1979) 775.
225 I.S. Gotkis, A.V. Gusarov, V.S. Pervov and V.D. Butskii, Koord. Khim., 4 (1978) 720.
226 G.V. Girichev, V.N. Petrova, V.M. Petrov, K.S. Krasnov and V.P. Goncharuk, Zh. Strukt. Khim., 24 (1983) 54.
227 K.A.R. Mitchell, Chem. Rev., 69 (1969) 157.
228 H.M. Seip and R. Seip, Acta Chem. Scand., 20 (1966) 2698.
229 M. Kimura, V. Schomaker, D.W. Smith and B. Weinstock, J. Chem. Phys., 48 (1968) 4001.
230 E.J. Jacob and L.S. Bartell, J. Chem. Phys., 53 (1970) 2231.
231 H.M. Seip, Acta Chem. Scand., 19 (1965) 1955.
232 H.H. Claassen, E.L. Gasner and H. Selig, J. Chem. Phys., 49 (1968) 1803; H.H. Claassen and H. Selig, J. Chem. Phys., 43 (1965) 103.
233 E.W. Kaiser, J.S. Muenter, W. Klemperer and W.E. Falconer, J. Chem. Phys., 53 (1970) 53.
234 E.J. Jacob and L.S. Bartell, J. Chem. Phys., 53 (1970) 2235.
235 M. Hargittai, Kem. Kozl., 50 (1978) 489.
236 G.I. Novikov and F.G. Gavryuchenkov, Uspek. Khim., 36 (1967) 399.
237 V.B. Solc and L.N. Sidorov, Vest. Mosk. Univ. Ser. Khim., 13 (1972) 371.
238 R. Huglen, S.J. Cyvin and H.A. Øye, Spectroscopic studies of alkali tetrafluoroaluminates, in D.L. Hildenbrand and D.D. Cubicciotti (Eds.), Proc. Symp. on High Temperature Metal Halide Chemistry, Electrochemical Society, Princeton, NJ, 1978, p. 352.
239 G.N. Papatheodorou, Spectroscopy, structure, and bonding of high temperature metal halide vapor complexes, in E. Kaldis (Ed.), Current Topics in Materials Science, Vol. 10, North-Holland, Amsterdam, 1982.
240 Yu.A. Brezgin, Thesis, Moscow State University, Moscow, 1972.
241 V.P. Spiridonov, E.V. Erokhin and Yu.A. Brezgin, Zh. Strukt. Khim., 13 (1972) 321.
242 V.P. Spiridonov, E.V. Erokhin and M.I. Shakhparonov, Zh. Strukt. Khim., 12 (1971) 1080.
243 V.P. Spiridonov, Yu.A. Brezgin and M.I. Shakhparonov, Zh. Strukt. Khim., 13 (1972) 320.
244 L.A. Curtiss, Chem. Phys. Lett., 68 (1979) 225.
245 V.P. Spiridonov and E.V. Erokhin, Zh. Neorg. Khim., 14 (1969) 636.
246 E. Vajda, I. Hargittai and J. Tremmel, Inorg. Chim. Acta, 25 (1977) L143.
247 Yu.Sh. Kalaichev, K.P. Petrov and V.V. Ugarov, Zh. Strukt. Khim., 24 (1983) 176.
248 Yu.Sh. Kalaichev, K.P. Petrov and V.V. Ugarov, Zh. Strukt. Khim., 24 (1983) 173.
249 Yu.Sh. Kalaichev, K.P. Petrov and V.V. Ugarov, Zh. Strukt. Khim., 24 (1983) 179.
250 V.P. Spiridonov, E.V. Erokhin and B.I. Lutoshkin, Vest. Mosk. Univ. Ser. Khim., 12 (1971) 296.
251 N.G. Rambidi, J. Mol. Struct., 28 (1975) 77, 88.

252 E. Rytter, H.A. Øye, S.J. Cyvin, B. Cyvin and P. Klaeboe, J. Inorg. Nucl. Chem., 35 (1973) 1185.
253 L.A. Curtiss and A. Heinricker, Int. J. Quantum Chem., 16 (1982) 285; Chem. Phys. Lett., 86 (1982) 467.